8 B-meson decay constants, mixing parameters and form factors

The (semi)leptonic decay and mixing processes of $B_{(s)}$ mesons have been playing a crucial role in flavour physics. In particular, they contain important information for the investigation of the $b-d$ unitarity triangle in the Cabibbo-Kobayashi-Maskawa (CKM) matrix, and can be ideal probes to physics beyond the Standard Model. The charged-current decay channels $B^+ \to l^+\nu_l$ and $B^0 \to \pi^- l^+\nu_l$, where l^+ is a charged lepton with ν_l being the corresponding neutrino, are essential in extracting the CKM matrix element $|V_{ub}|$. Similarly, the B to $D^{(*)}$ semileptonic transitions can be used to determine $|V_{cb}|$. The flavour changing neutral current (FCNC) processes, such as $B \to K^{(*)}\ell^+\ell^-$ and $B_{d(s)} \to \ell^+\ell^-$, occur only beyond the tree level in weak interactions and are suppressed in the Standard Model. Therefore, these processes can be sensitive to new physics, since heavy particles can contribute to the loop diagrams. They are also suitable channels for the extraction of the CKM matrix elements involving the top quark which can appear in the loop. For instance, the neutral $B_{d(s)}$-meson mixings are FCNC processes and are dominated by the 1-loop "box" diagrams containing the top quark and the W bosons. Thus, using the experimentally measured neutral $B^0_{d(s)}$-meson oscillation frequencies, $\Delta M_{d(s)}$, and the theoretical calculations for the relevant hadronic mixing matrix elements, one can obtain $|V_{td}|$ and $|V_{ts}|$ in the Standard Model.[1]

Accommodating the light quarks and the b quark simultaneously in lattice-QCD computations is a challenging endeavour. To incorporate the pion and the b hadrons with their physical masses, the simulations have to be performed using the lattice size $\hat{L} = L/a \sim \mathcal{O}(10^2)$, where a is the lattice spacing and L is the physical (dimensionful) box size. This is a few times larger than what one can practically afford in contemporary numerical projects. Therefore, in addition to employing Chiral Perturbation Theory for the extrapolations in the light-quark mass, current lattice calculations for quantities involving b hadrons often make use of effective theories that allow one to expand in inverse powers of m_b. In this regard, two general approaches are widely adopted. On the one hand, effective field theories such as Heavy-Quark Effective Theory (HQET) and Nonrelativistic QCD (NRQCD) can be directly implemented in numerical computations. On the other hand, a relativistic quark action can be improved *á la* Symanzik to suppress cutoff errors, and then re-interpreted in a manner that is suitable for heavy-quark physics calculations. This latter strategy is often referred to as the method of the Relativistic Heavy-Quark Action (RHQA). The utilization of such effective theories inevitably introduces systematic uncertainties that are not present in light-quark calculations. These uncertainties can arise from the truncation of the expansion in constructing the effective theories (as in HQET and NRQCD), or from more intricate cutoff effects (as in NRQCD and RQHA). They can also be introduced through more complicated renormalization procedures which often lead to significant systematic effects in matching the lattice operators to their continuum counterparts. For instance, due to the use of different actions for the heavy and the light quarks, it is more difficult to construct absolutely normalized bottom-light currents.

Complementary to the above "effective theory approaches", another popular method is to simulate the heavy and the light quarks using the same (normally improved) lattice action at several values of the heavy-quark mass, m_h, with $am_h < 1$ and $m_h < m_b$. This enables one

[1] The neutral B-meson leptonic decays, $B_{d,s} \to \mu^+\mu^-$, were recently observed at the LHC experiments, and the corresponding branching fractions can be obtained by combining the data from the CMS and the LHCb collaborations [1]. Nevertheless, the errors of these experimental results are currently too large to enable a precise determination of $|V_{td}|$ and $|V_{ts}|$.

to employ HQET-inspired relations to extrapolate the computed quantities to the physical b mass. When combined with results obtained in the static heavy-quark limit, this approach can be rendered into an interpolation, instead of extrapolation, in m_h. The discretization errors are the main source of the systematic effects in this method, and very small lattice spacings are needed to keep such errors under control.

Because of the challenge described above, the efforts that have been made to obtain reliable, accurate lattice-QCD results for physics of the b quark have been enormous. These efforts include significant theoretical progress in formulating QCD with heavy quarks on the lattice. This aspect is briefly reviewed in Appendix A.1.3.

In this section, we summarize the results of the B-meson leptonic decay constants, the neutral B-mixing parameters, and the semileptonic form factors, from lattice QCD. To be focused on the calculations which have strong phenomenological impact, we limit the review to results based on modern simulations containing dynamical fermions with reasonably light pion masses (below approximately 500 MeV). Compared to the progress in the light-quark sector, heavy-quark physics on the lattice is not as mature. Consequently, fewer collaborations have finished calculations for these quantities. In addition, the existing results are often obtained at coarser lattice spacings and heavier pions. Therefore, for some quantities, there is only a single lattice calculation that satisfies the criteria to be included in our average. Nevertheless, several collaborations are currently pursuing this line of research with various lattice b-quark actions, finer lattice spacings, and lighter pions. Thus many new results with controlled errors are expected to appear in the near future.

Following our review of $B_{(s)}$-meson leptonic decay constants, the neutral B-meson mixing parameters, and semileptonic form factors, we then interpret our results within the context of the Standard Model. We combine our best-determined values of the hadronic matrix elements with the most recent experimentally-measured branching fractions to obtain $|V_{(u)cb}|$ and compare these results to those obtained from inclusive semileptonic B decays.

Recent lattice-QCD averages for B^+- and B_s-meson decay constants were also presented by the Particle Data Group (PDG) in Ref. [2]. The PDG three- and four-flavour averages for these quantities differ from those quoted here because the PDG provides the charged-meson decay constant, f_{B^+}, while we present the isospin-averaged meson-decay constant, f_B.

8.1 Leptonic decay constants f_B and f_{B_s}

The B and B_s meson decay constants are crucial input for extracting information from leptonic B decays. Charged B mesons can decay to the lepton-neutrino final state through the charged-current weak interaction. On the other hand, neutral $B_{d(s)}$ mesons can decay to a charged-lepton pair via a flavour-changing neutral current (FCNC) process.

In the Standard Model the decay rate for $B^+ \to \ell^+\nu_\ell$ is described by a formula identical to Eq. (128), with $D_{(s)}$ replaced by B, and the relevant CKM matrix element, V_{cq}, substituted by V_{ub},

$$\Gamma(B \to \ell\nu_\ell) = \tfrac{m_B}{8\pi} G_F^2 f_B^2 |V_{ub}|^2 m_\ell^2 \left(1 - \tfrac{m_\ell^2}{m_B^2}\right)^2 . \tag{150}$$

The only charged-current B meson decay that has been observed so far is $B^+ \to \tau^+\nu_\tau$, which has been measured by the Belle and Babar collaborations [3, 4]. Both collaborations have reported results with errors around 20%. These measurements can be used to determine $|V_{ub}|$ when combined with lattice-QCD predictions of the corresponding decay constant.

Neutral $B_{d(s)}$-meson decays to a charged lepton pair, $B_{d(s)} \to l^+l^-$ is a FCNC process, and can only occur at 1-loop in the Standard Model. Hence these processes are expected to be rare, and are sensitive to physics beyond the Standard Model. The corresponding expression for the branching fraction has the form

$$B(B_q \to \ell^+\ell^-) = \frac{\tau_{B_q}}{1+y_q}\frac{G_F^2\alpha^2}{16\pi^3} m_{B_q} f_{B_q}^2 |V_{tb}^* V_{tq}|^2 m_\ell^2 C_{10}^{\rm SM} \sqrt{1-\frac{4m_\ell^2}{m_{B_q}^2}}, \tag{151}$$

where the light-quark $q = s$ or d, and the coefficient $C_{10}^{\rm SM}$ includes the NLO electro-weak and NNLO QCD matching corrections [5]. The factor $1/(1+y_q)$, with $y_q = \Delta\Gamma_{B_q}/(2\Gamma_{B_q})$, accounts for the fact that the measured branching fraction corresponds to a time-integrated rate of the oscillating B_q system to $\ell^+\ell^-$ [6]. That correction is particularly important for the B_s decays because of the relatively large $y_s = 0.06(1)$ [7, 8]. Evidence for both $B_s \to \mu^+\mu^-$ and $B_s \to \mu^+\mu^-$ decays was recently observed by the CMS and the LHCb collaborations. Combining the data from both collaborations, the branching fractions can be extracted to be [1],

$$\begin{aligned} B(B_d \to \mu^+\mu^-) &= (3.9^{+1.6}_{-1.4})\,10^{-10}, \\ B(B_s \to \mu^+\mu^-) &= (2.8^{+0.7}_{-0.6})\,10^{-9}, \end{aligned} \tag{152}$$

which are compatible with the Standard Model predictions at the 2.2σ and 1.2σ level, respectively.

The decay constants f_{B_q} (with $q = u, d, s$) parameterize the matrix elements of the corresponding axial-vector currents, $A_{bq}^\mu = \bar{b}\gamma^\mu\gamma^5 q$, analogously to the definition of f_{D_q} in Sec. 7.1:

$$\langle 0|A^\mu|B_q(p)\rangle = ip_B^\mu f_{B_q}\ . \tag{153}$$

For heavy-light mesons, it is convenient to define and analyze the quantity

$$\Phi_{B_q} \equiv f_{B_q}\sqrt{m_{B_q}}\ , \tag{154}$$

which approaches a constant (up to logarithmic corrections) in the $m_B \to \infty$ limit according to HQET. In the following discussion we denote lattice data for $\Phi(f)$ obtained at a heavy-quark mass m_h and light valence-quark mass m_ℓ as $\Phi_{h\ell}(f_{hl})$, to differentiate them from the corresponding quantities at the physical b and light-quark masses.

The $SU(3)$-breaking ratio, f_{B_s}/f_B, is of interest. This is because in lattice-QCD calculations for this quantity, many systematic effects can be partially reduced. These include discretization errors, heavy-quark mass tuning effects, and renormalization/matching errors, amongst others. On the other hand, this $SU(3)$-breaking ratio is still sensitive to the chiral extrapolation. Given that the chiral extrapolation is under control, one can then adopt f_{B_s}/f_B as input in extracting phenomenologically-interesting quantities. For instance, this ratio can be used to determine $|V_{ts}/V_{td}|$. In addition, it often happens to be easier to obtain lattice results for f_{B_s} with smaller errors. Therefore, one can combine the B_s-meson decay constant with the $SU(3)$-breaking ratio to calculate f_B. Such strategy can lead to better precision in the computation of the B-meson decay constant, and has been adopted by the ETM [9] and the HPQCD collaborations [10].

It is clear that the decay constants for charged and neutral B mesons play different roles in flavour physics phenomenology. As already mentioned above, the knowledge of the B^+-meson

decay constant, f_{B^+}, is essential for extracting $|V_{ub}|$ from leptonic B^+ decays. The neutral B-meson decay constants, f_{B^0} and f_{B_s}, are inputs for obtaining $|V_{td}|$ using information from the B-meson mixing processes. In view of this, it is desirable to include isospin-breaking effects in lattice computations for these quantities, and have results for f_{B^+} and f_{B^0}. Nevertheless, as will be discussed in detail in this section, such effects are small compared to the current errors of the decay constants calculated using lattice QCD. In this review, we will then concentrate on the isospin-averaged result, f_B, and the B_s-meson decay constant, as well as the $SU(3)$-breaking ratio, f_{B_s}/f_B. For the world average for the lattice determination of f_{B^+} and f_{B_s}/f_{B^+}, we refer the reader to the latest work from the Particle Data Group (PDG) [2]. Notice that the lattice results used in Ref. [2] and the current review are identical. We will discuss this in further detail at the end of this subsection.

The status of lattice-QCD computations for B-meson decay constants and the $SU(3)$-breaking ratio, using gauge-field ensembles with light dynamical fermions, is summarized in Tabs. 32 and 33. Figs. 20 and 21 contain the graphic presentation of the collected results and our averages. Many results in these tables and plots were already reviewed in detail in the previous FLAG report [11]. Below we will describe the new results that appeared after December 2013. In addition, we will comment on our updated strategies in performing the averaging.

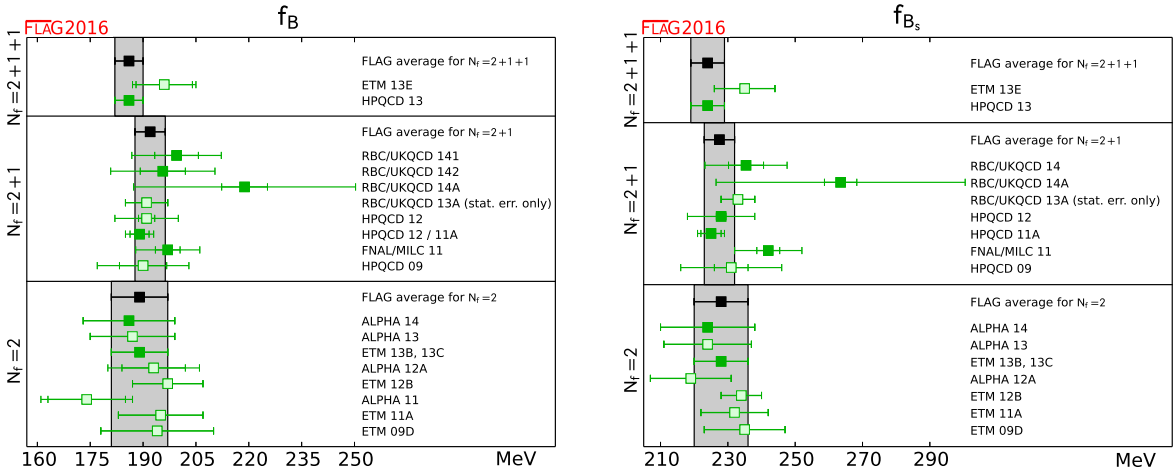

Figure 20: Decay constants of the B and B_s mesons. The values are taken from Tab. 32 (the f_B entry for FNAL/MILC 11 represents f_{B^+}). The significance of the colours is explained in Sec. 2. The black squares and grey bands indicate our averages in Eqs. (155), (156) and (157).

Only one new $N_f = 2$ project for computing f_B, f_{B_s} and f_{B_s}/f_B was completed after the publication of the previous FLAG review. This was carried out by the ALPHA collaboration [20] (ALPHA 14 in Tabs. 32 and 33), on the CLS (Coordinated Lattice Simulations) gauge-field ensembles which were generated using the Wilson plaquette action and $N_f = 2$ non-perturbatively $\mathcal{O}(a)$-improved Wilson fermions with the DD-HMC [30–32] or the MP-HMC [33] algorithm. There are three choices of lattice spacing, 0.048, 0.065 and 0.075 fm, in these ensembles. At each lattice spacing, three to four lattice sizes are adopted in the simula-

Collaboration	Ref.	N_f	publication status	continuum extrapolation	chiral extrapolation	finite volume	renormalization/matching	heavy-quark treatment	f_{B^+}	f_{B^0}	f_B	f_{B_s}
ETM 13E	[12]	2+1+1	C	○	○	○	○	✓	–	–	196(9)	235(9)
HPQCD 13	[13]	2+1+1	A	★	★	★	○	✓	184(4)	188(4)	186(4)	224(5)
RBC/UKQCD 14	[14]	2+1	A	○	○	○	○	✓	195.6(14.9)	199.5(12.6)	–	235.4(12.2)
RBC/UKQCD 14A	[15]	2+1	A	○	○	○	○	✓	–	–	219(31)	264(37)
RBC/UKQCD 13A	[16]	2+1	C	○	○	○	○	✓	–	–	$191(6)^{\diamond}_{\text{stat}}$	$233(5)^{\diamond}_{\text{stat}}$
HPQCD 12	[10]	2+1	A	○	○	○	○	✓	–	–	191(9)	228(10)
HPQCD 12	[10]	2+1	A	○	○	○	○	✓	–	–	$189(4)^{\triangle}$	–
HPQCD 11A	[17]	2+1	A	★	○	★	★	✓	–	–	–	$225(4)^{\nabla}$
FNAL/MILC 11	[18]	2+1	A	○	○	★	○	✓	197(9)	–	–	242(10)
HPQCD 09	[19]	2+1	A	○	○	○	○	✓	–	–	$190(13)^{\bullet}$	$231(15)^{\bullet}$
ALPHA 14	[20]	2	A	★	★	★	★	✓	–	–	186(13)	224(14)
ALPHA 13	[21]	2	C	★	★	★	★	✓	–	–	187(12)(2)	224(13)
ETM 13B, 13C†	[9, 22]	2	A	★	○	★	○	✓	–	–	189(8)	228(8)
ALPHA 12A	[23]	2	C	★	★	★	★	✓	–	–	193(9)(4)	219(12)
ETM 12B	[24]	2	C	★	○	★	○	✓	–	–	197(10)	234(6)
ALPHA 11	[25]	2	C	★	○	★	★	✓	–	–	174(11)(2)	–
ETM 11A	[26]	2	A	○	○	★	○	✓	–	–	195(12)	232(10)
ETM 09D	[27]	2	A	○	○	○	○	✓	–	–	194(16)	235(12)

$^{\diamond}$ Statistical errors only.
$^{\triangle}$ Obtained by combining f_{B_s} from HPQCD 11A with f_{B_s}/f_B calculated in this work.
$^{\nabla}$ This result uses one ensemble per lattice spacing with light to strange sea-quark mass ratio $m_\ell/m_s \approx 0.2$.
$^{\bullet}$ This result uses an old determination of $r_1 = 0.321(5)$ fm from Ref. [28] that has since been superseded.
† Update of ETM 11A and 12B.

Table 32: Decay constants of the B, B^+, B^0 and B_s mesons (in MeV). Here f_B stands for the mean value of f_{B^+} and f_{B^0}, extrapolated (or interpolated) in the mass of the light valence-quark to the physical value of m_{ud}.

tions. The hyper-cubic boxes are of the shape $L^3 \times T$, with the temporal extent $T = 2L$. The smallest box used in ALPHA 14 is $L \approx 2$ fm. On each of these lattice sizes, one sea-quark mass is employed in the computation, and the condition $M_\pi L > 4$ is always ensured. This leads to subpercentage-level finite-size effects [34]. The corresponding lightest pions composed of the sea quarks for these three values of the lattice spacing are 270, 190, and 280 MeV, respectively. In this work, the lattice-regularized HQET action and the axial current to the order of $1/m_B$, as tuned in Refs. [35–39] with non-perturbative matching to QCD, are used to compute the heavy-light meson decay constant. This matching procedure removes both the logarithmic

Collaboration	Ref.	N_f	publication status	continuum extrapolation	chiral extrapolation	finite volume	renormalization/matching	heavy-quark treatment	f_{B_s}/f_{B^+}	f_{B_s}/f_{B^0}	f_{B_s}/f_B
ETM 13E	[12]	2+1+1	C	★	○	○	○	✓	–	–	1.201(25)
HPQCD 13	[13]	2+1+1	A	★	★	★	○	✓	1.217(8)	1.194(7)	1.205(7)
RBC/UKQCD 14	[14]	2+1	A	○	○	○	○	✓	1.223(71)	1.197(50)	–
RBC/UKQCD 14A	[15]	2+1	A	○	○	○	○	✓	–	–	1.193(48)
RBC/UKQCD 13A	[16]	2+1	C	○	○	○	○	✓	–	–	$1.20(2)^{\diamond}_{\text{stat}}$
HPQCD 12	[10]	2+1	A	○	○	○	○	✓	–	–	1.188(18)
FNAL/MILC 11	[18]	2+1	A	○	○	★	○	✓	1.229(26)	–	–
RBC/UKQCD 10C	[29]	2+1	A	■	■	■	○	✓	–	–	1.15(12)
HPQCD 09	[19]	2+1	A	○	○	○	○	✓	–	–	1.226(26)
ALPHA 14	[20]	2	A	★	★	★	★	✓	–	–	1.203(65)
ALPHA 13	[21]	2	C	★	★	★	★	✓	–	–	1.195(61)(20)
ETM 13B, 13C†	[9, 22]	2	A	★	○	★	○	✓	–	–	1.206(24)
ALPHA 12A	[23]	2	C	★	★	★	★	✓	–	–	1.13(6)
ETM 12B	[24]	2	C	★	○	★	○	✓	–	–	1.19(5)
ETM 11A	[26]	2	A	○	○	★	○	✓	–	–	1.19(5)

$^{\diamond}$ Statistical errors only.
† Update of ETM 11A and 12B.

Table 33: Ratios of decay constants of the B and B_s mesons (for details see Tab. 32).

and the power divergences in the effective theory regularized on the lattice. The valence light (up and down) quarks are implemented with the unitary setup, such that the valence and the sea pions have identical masses. On the other hand, the valence strange-quark mass is tuned on the CLS gauge-field ensembles employing the kaon decay constant [40]. The static-light axial current in this work is also $\mathcal{O}(a)$-improved to 1-loop order. Using the lattice data, the ground-state contributions to the relevant correlators are obtained through the method of the generalized eigenvalue problem (GEVP), as detailed in Ref. [41]. With this GEVP approach in ALPHA 14, the systematic errors arising from the excited-state contamination are typically less than one third of the statistical errors in the extracted decay constants. Combined chiral-continuum extrapolations, adopting the NLO HMχPT predictions, are then performed to determine the decay constants in the limit of physical pion mass and vanishing lattice spacing. The errors of the final results in ALPHA 14 include statistical uncertainties, the discrepancy to the static-limit results, the effects of the lattice spacing, the uncertainties from the HQET parameters in the matching procedure, and the systematic effects in the chiral

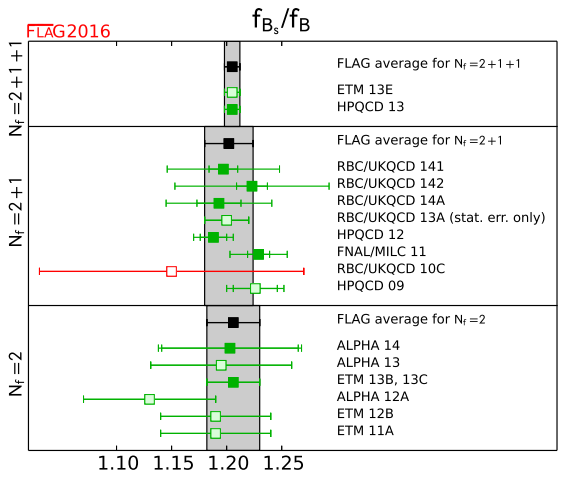

Figure 21: Ratio of the decay constants of the B and B_s mesons. The values are taken from Tab. 33 (the f_B entry for FNAL/MILC 11 represents f_{B^+}). The significance of the colours is explained in Sec. 2. The black squares and grey bands indicate our averages in Eqs. (155), (156) and (157).

extrapolations as estimated by comparing with fits to formulae without the chiral logarithms. Since the fits to the predictions of finite-volume HMχPT [34] have not been implemented, systematic effects resulting from the finite lattice size are not included in the analysis. Nevertheless, given that the condition $M_\pi L > 4$ is always satisfied in ALPHA 14, these effects should be at the subpercentage level according to the 1-loop formulae in Ref. [34].

The new result, ALPHA 14, satisfies all our criteria for being included in the averaging process. Therefore, in the current edition of the FLAG report, two $N_f = 2$ calculations for the B-meson decay constants and the $SU(3)$-breaking ratio contribute to our averages. The other determination of these quantities (ETM 13B, 13C in Tabs. 32 and 33) was already reviewed in detail in the previous FLAG publication. These two projects are based on completely different lattice simulations, and there is no correlation between the errors quoted in them. This gives our estimate,

$$N_f = 2: \quad \begin{aligned} f_B &= 188(7)\ \text{MeV} && \text{Refs. [9, 20, 22]}, \\ f_{B_s} &= 227(7)\ \text{MeV} && \text{Refs. [9, 20, 22]}, \\ f_{B_s}/f_B &= 1.206(23) && \text{Refs. [9, 20, 22]}. \end{aligned} \tag{155}$$

Two groups of authors (RBC/UKQCD 14 [14] and RBC/UKQCD 14A [15] in Tabs. 32 and 33) presented their $N_f = 2+1$ results for f_B, f_{B_s} and f_{B_s}/f_B after the publication of the previous FLAG report in 2013. Both groups belong to the RBC/UKQCD collaboration. They use the same gauge-field ensembles generated by this collaboration, with the Iwasaki gauge action and domain-wall dynamical quarks [42], adopting the "RHMC II" algorithm [43]. Two values of the lattice spacing, 0.11 and 0.086 fm, are used in the simulations, with the corresponding lattice sizes being $24^3 \times 64$ and $32^3 \times 64$, respectively. This fixes the spatial size $L \approx 2.7$ fm in all the data sets. For the coarse lattice, two choices of the sea-quark masses, with $M_\pi \approx 328$ and 420 MeV, are implemented in the simulations. On the other hand, three

values of the sea-quark masses ($M_\pi \approx 289$, 344, 394 MeV) are used on the fine lattice. This makes certain that $M_\pi L > 4$ is always satisfied. At each value of the lattice spacing, only one sea strange-quark mass is implemented, which is about 10% higher than its physical value.

In RBC/UKQCD 14, the heavy-quark is described by the relativistic lattice action proposed in Ref. [44]. The three parameters of this relativistic heavy-quark (RHQ) action are tuned non-perturbatively in Ref. [45] by requiring that the spin-averaged B_s-meson mass, $\overline{M}_{B_s} = (M_{B_s} + 3M_{B_s^*})/4$, and the hyperfine splitting, $\Delta_{M_{B_s}} = M_{B_s^*} - M_{B_s}$ equal the PDG values, and that the lattice rest and kinetic meson masses are equal. Statistical uncertainties in the tuned parameters are propagated to the decay constants via jackknife resampling. Simulations with different values of the RHQ parameters are used to estimate the remaining uncertainties in the decay constants from the tuning procedure. Regarding valence light- and strange-quarks, the authors of RBC/UKQCD 14 adopt exactly the same domain-wall discretization as that in the sea-quark sector. For each lattice spacing, such valence domain-wall fermion propagators at six choices of the mass parameter are generated. These six values straddle between the lightest and strange sea-quark masses in the gauge-field ensembles, and several of them correspond to the unitary points. With the above lattice setting, the heavy-meson decay constants are obtained, employing an axial current that is $\mathcal{O}(a)$-improved to 1-loop level. The renormalization of the axial current is carried out with a mostly nonperturbative procedure proposed in Ref. [46]. Linear interpolations for the heavy-quark action parameters, as well as the valence strange-quark mass are then performed on these heavy-meson decay constants. As for the chiral extrapolation for the light-quark mass, it is implemented together with the continuum extrapolation (linear in a^2) adopting $SU(2)$-HMχPT at NLO.[2] The decay constants, f_{B^+} and f_{B^0}, are determined by chirally extrapolating to the physical u- and d-quark masses, respectively, and their isospin-averaged counterpart, f_B, is not reported. Notice that only the unitary points in the light-quark mass are used in the central procedure for the chiral extrapolation. This extrapolation serves as the method to confirm that finite-size effects are at the subpercentage level by comparing with the prediction of finite-volume HMχPT [34]. Furthermore, since there is no observed sea-quark dependence in f_{B_s}, it is extrapolated to the continuum limit straight after the interpolation of the valence strange-quark mass. The authors of RBC/UKQCD 14 provided a comprehensive list of systematic errors in their work. The dominant effect is from the chiral-continuum extrapolation. This was investigated using several alternative procedures by varying the fit ansätze and omitting the data points at the heaviest pion mass. The error arising from the continuum extrapolation of f_{B_s} is estimated by taking the result on the finer lattice as the alternative. One other important source of the systematic errors is the heavy-quark discretization effect, which is estimated using a power-counting argument in the improvement programme.

In the other newly completed B-meson decay constants project, RBC/UKQCD 14A, the static heavy-quark action is implemented with the HYP smearing [47] that reduces the power divergences. As for the valence light- and strange-quarks, the same domain-wall discretization as adopted for the sea quarks is used. The masses of the valence light quarks are chosen to be at the unitary points. On the other hand, for each lattice spacing, two values of the valence strange-quark mass are utilized, with one of them identical to that of its sea-quark

[2] The authors of RBC/UKQCD 14 claim that using the NLO $SU(3)$-HMχPT extrapolation formulae, acceptable fits for the decay constants can be found. On the other hand, no reasonable fit for the ratio, f_{B_s}/f_B, can result from this procedure, because this ratio has smaller statistical errors. The NLO $SU(3)$-HMχPT predictions are then used as a means to estimate the systematic effects arising from the chiral-continuum extrapolation.

counterpart, and the other slightly smaller than the physical strange-quark mass. Employing the propagators of these valence quarks computed on the RBC/UKQCD gauge-field ensembles, the relevant matrix elements of the axial current are calculated to extract the decay constant. Notice that the source and sink smearings are applied on the valence light- and strange-quark propagators, in order to obtain better overlap with the ground state. The axial current is $\mathcal{O}(a)$-improved to 1-loop order, and its renormalization/matching is performed in a two-step fashion. Namely, it is first matched from the lattice-regularized HQET to the same effective theory in the continuum at the inverse lattice spacing, a^{-1}, and then matched to QCD at the physical b-quark mass, m_b. At each of these two steps, the matching is carried out at 1-loop level, and the 2-loop running between a^{-1} and m_b is implemented accordingly. Regarding the extrapolation to the physical light-quark mass, it is achieved using $SU(2)$-HMχPT, after linearly interpolating the decay constants to the physical strange-quark mass in the valence sector. Unlike RBC/UKQCD 14, here the isospin-averaged f_B, instead of the individual f_{B^+} and f_{B^0}, is reported in RBC/UKQCD 14A. This chiral fit is combined with the continuum extrapolation by including a term proportional to a^2 in the HMχPT formulae. In addition, finite-size effects are also estimated by replacing the 1-loop integrals with sums in HMχPT [34]. The predominant systematic error in f_{B_s} and f_B is from the 1-loop renormalization/matching procedure. This error is accounted for by employing a power-counting method, and is evaluated to be around 6%. Obviously, it is small for f_{B_s}/f_B. Another significant systematic effect (about 2 $\sim$ 3% in all relevant quantities) results from the chiral-continuum extrapolation. This effect is estimated by omitting the chiral logarithms in the fitting procedure. Finally, based upon a power-counting argument, the authors of RBC/UKQCD 14A include a 10% error on $f_{B_{(s)}}$, and a 2.2% error on f_{B_s}/f_B, to account for the use of the static heavy quarks in their work.

Both new computations from the RBC/UKQCD collaboration satisfy the criteria for being considered in our averages of the relevant quantities. Since they are based on exactly the same gauge-field configurations, we treat the statistical errors in these two results as 100% correlated. It also has to be pointed out that only f_{B^+} and f_{B^0} are reported in RBC/UKQCD 14, while we are concentrating on the isospin-averaged f_B in our current work. For this purpose, we regard both f_{B^+} and f_{B^0} in RBC/UKQCD 14 as f_B, and completely correlate all the errors.

In addition to RBC/UKQCD 14 and RBC/UKQCD 14A, a few other results in Tabs. 32 and 33 are also in our averaging procedure. These include HPQCD 12, HPQCD 11A, and FNAL/MILC 11. Notice that there are two results of f_B from HPQCD 12 in Tab. 32. Both of these were in the averaging procedure in the last edition of the FLAG report. However, for our current work, we only include the one with smaller error. This result is obtained by taking f_{B_s}/f_B computed with the NRQCD description of the b quark in HPQCD 12, and multiplying it by f_{B_s} calculated employing the HISQ discretization for the heavy quarks in HPQCD 11A. This strategy significantly reduces the systematic effect arising from the renormalization of the axial current in Eq. (153), as compared to the "direct" determination of f_B using NRQCD heavy quarks in HPQCD 12. Since the calculations performed in FNAL/MILC 11, HPQCD 12 and HPQCD 11A all involve the gauge-field ensembles generated by the MILC collaboration, we treat their statistical errors as 100% correlated. Following the above discussion, our

procedure leads to the averages,

$$N_f = 2+1: \quad \begin{aligned} f_B &= 192.0(4.3)\ \text{MeV} && \text{Refs. [10, 14, 15, 17, 18]},\\ f_{B_s} &= 228.4(3.7)\ \text{MeV} && \text{Refs. [10, 14, 15, 17, 18]},\\ f_{B_s}/f_B &= 1.201(16) && \text{Refs. [10, 14, 15, 18]}. \end{aligned} \tag{156}$$

There have been no new $N_f = 2+1+1$ results for the B-meson decay constants and the $SU(3)$-breaking ratio since the release of the previous FLAG publication.[3] Therefore, our averages remain the same as those in the previous FLAG report,

$$N_f = 2+1+1: \quad \begin{aligned} f_B &= 186(4)\ \text{MeV} && \text{Refs. [13]},\\ f_{B_s} &= 224(5)\ \text{MeV} && \text{Refs. [13]},\\ f_{B_s}/f_B &= 1.205(7) && \text{Refs. [13]}. \end{aligned} \tag{157}$$

The PDG recently presented their averages for the $N_f = 2+1$ and $N_f = 2+1+1$ lattice-QCD determinations of f_{B^+}, f_{B_s} and f_{B_s}/f_{B^+} [2].[4] The lattice-computation results used in Ref. [2] are identical to those included in our current work. Regarding our isospin-averaged f_B as the representative for f_{B^+}, then the results from current FLAG and PDG estimations for these quantities are well compatible. In the PDG work, they "corrected" the isospin-averaged f_B, as reported by various lattice collaborations, using the $N_f = 2+1+1$ strong isospin-breaking effect computed in HPQCD 13 [13] (see Tab. 32 in this subsection). This only accounts for the contribution from the valence-quark masses. However, since the isospin-breaking effects from the sea-quark masses appear in the form $(m_u^{(\text{sea})} - m_d^{(\text{sea})})^2$, the valence sector is the predominant source of strong isospin breaking [49].[5]

8.2 Neutral B-meson mixing matrix elements

Neutral B-meson mixing is induced in the Standard Model through 1-loop box diagrams to lowest order in the electroweak theory, similar to those for short-distance effects in neutral kaon mixing. The effective Hamiltonian is given by

$$\mathcal{H}_{\text{eff}}^{\Delta B=2,\text{SM}} \;=\; \tfrac{G_F^2 M_W^2}{16\pi^2}(\mathcal{F}_d^0 \mathcal{Q}_1^d + \mathcal{F}_s^0 \mathcal{Q}_1^s) \;+\; \text{h.c.}\,, \tag{158}$$

with

$$\mathcal{Q}_1^q = \left[\bar{b}\gamma_\mu(1-\gamma_5)q\right]\left[\bar{b}\gamma_\mu(1-\gamma_5)q\right], \tag{159}$$

where $q = d$ or s. The short-distance function $\mathcal{F}_q^0$ in Eq. (158) is much simpler compared to the kaon mixing case due to the hierarchy in the CKM matrix elements. Here, only one term is relevant,

$$\mathcal{F}_q^0 = \lambda_{tq}^2 S_0(x_t) \tag{160}$$

where

$$\lambda_{tq} = V_{tq}^* V_{tb}, \tag{161}$$

[3] At the Lattice 2015 conference, the Fermilab Lattice and MILC collaborations reported their on-going project for computing the B-meson decay constants in $N_f = 2+1+1$ QCD [48]. However, no result has been shown yet.

[4] We thank Ruth Van de Water for communication and discussion regarding the comparison of the averaging strategies.

[5] We thank Ruth Van de Water and Andre Walker-Loud for helpful discussion on this point.

and where $S_0(x_t)$ is an Inami-Lim function with $x_t = m_t^2/M_W^2$, which describes the basic electroweak loop contributions without QCD [50]. The transition amplitude for B_q^0 with $q = d$ or s can be written as

$$\begin{aligned}\langle \bar{B}_q^0|\mathcal{H}_{\rm eff}^{\Delta B=2}|B_q^0\rangle \;&=\; \tfrac{G_F^2 M_{\rm W}^2}{16\pi^2}\Big[\lambda_{tq}^2 S_0(x_t)\eta_{2B}\Big] \\ \times\left(\tfrac{\bar{g}(\mu)^2}{4\pi}\right)^{-\gamma_0/(2\beta_0)} &\exp\left\{\int_0^{\bar{g}(\mu)} dg\left(\tfrac{\gamma(g)}{\beta(g)} + \tfrac{\gamma_0}{\beta_0 g}\right)\right\}\langle \bar{B}_q^0|Q_{\rm R}^q(\mu)|B_q^0\rangle \;+\; \text{h.c.}\,, \end{aligned} \tag{162}$$

where $Q_{\rm R}^q(\mu)$ is the renormalized four-fermion operator (usually in the NDR scheme of $\overline{\rm MS}$). The running coupling ($\bar{g}$), the β-function ($\beta(g)$), and the anomalous dimension of the four-quark operator ($\gamma(g)$) are defined in Eqs. (104) and (105). The product of μ dependent terms on the second line of Eq. (162) is, of course, μ-independent (up to truncation errors arising from the use of perturbation theory). The explicit expression for the short-distance QCD correction factor η_{2B} (calculated to NLO) can be found in Ref. [51].

For historical reasons the B-meson mixing matrix elements are often parameterized in terms of bag parameters defined as

$$B_{B_q}(\mu) = \frac{\langle \bar{B}_q^0|Q_{\rm R}^q(\mu)|B_q^0\rangle}{\frac{8}{3} f_{B_q}^2 m_{\rm B}^2}\;. \tag{163}$$

The RGI B parameter $\hat{B}$ is defined as in the case of the kaon, and expressed to 2-loop order as

$$\hat{B}_{B_q} = \left(\tfrac{\bar{g}(\mu)^2}{4\pi}\right)^{-\gamma_0/(2\beta_0)}\left\{1 + \frac{\bar{g}(\mu)^2}{(4\pi)^2}\left[\tfrac{\beta_1\gamma_0 - \beta_0\gamma_1}{2\beta_0^2}\right]\right\} B_{B_q}(\mu)\;, \tag{164}$$

with β_0, β_1, γ_0, and γ_1 defined in Eq. (106). Note, as Eq. (162) is evaluated above the bottom threshold ($m_b < \mu < m_t$), the active number of flavours here is $N_f = 5$.

Nonzero transition amplitudes result in a mass difference between the CP eigenstates of the neutral B-meson system. Writing the mass difference for a B_q^0 meson as Δm_q, its Standard Model prediction is

$$\Delta m_q = \tfrac{G_F^2 m_W^2 m_{B_q}}{6\pi^2}\,|\lambda_{tq}|^2 S_0(x_t)\eta_{2B} f_{B_q}^2 \hat{B}_{B_q}. \tag{165}$$

Experimentally the mass difference is measured as oscillation frequency of the CP eigenstates. The frequencies are measured precisely with an error of less than a percent. Many different experiments have measured Δm_d, but the current average [52] is based on measurements from the B-factory experiments Belle and Babar, and from the LHC experiment LHCb. For Δm_s the experimental average is dominated by results from LHCb [52]. With these experimental results and lattice-QCD calculations of $f_{B_q}^2\hat{B}_{B_q}$ at hand, λ_{tq} can be determined. In lattice-QCD calculations the flavour $SU(3)$-breaking ratio

$$\xi^2 = \frac{f_{B_s}^2 B_{B_s}}{f_{B_d}^2 B_{B_d}} \tag{166}$$

can be obtained more precisely than the individual B_q-mixing matrix elements because statistical and systematic errors cancel in part. With this the ratio $|V_{td}/V_{ts}|$ can be determined, which can be used to constrain the apex of the CKM triangle.

Neutral B-meson mixing, being loop-induced in the Standard Model is also a sensitive probe of new physics. The most general $\Delta B = 2$ effective Hamiltonian that describes contributions to B-meson mixing in the Standard Model and beyond is given in terms of five local four-fermion operators:

$$\mathcal{H}_{\text{eff,BSM}}^{\Delta B=2} = \sum_{q=d,s} \sum_{i=1}^{5} \mathcal{C}_i \mathcal{Q}_i^q \,, \tag{167}$$

where $\mathcal{Q}_1$ is defined in Eq. (159) and where

$$\mathcal{Q}_2^q = \left[\bar{b}(1-\gamma_5)q\right]\left[\bar{b}(1-\gamma_5)q\right], \qquad \mathcal{Q}_3^q = \left[\bar{b}^\alpha(1-\gamma_5)q^\beta\right]\left[\bar{b}^\beta(1-\gamma_5)q^\alpha\right],$$
$$\mathcal{Q}_4^q = \left[\bar{b}(1-\gamma_5)q\right]\left[\bar{b}(1+\gamma_5)q\right], \qquad \mathcal{Q}_5^q = \left[\bar{b}^\alpha(1-\gamma_5)q^\beta\right]\left[\bar{b}^\beta(1+\gamma_5)q^\alpha\right], \tag{168}$$

with the superscripts α, β denoting colour indices, which are shown only when they are contracted across the two bilinears. There are three other basis operators in the $\Delta B = 2$ effective Hamiltonian. When evaluated in QCD, however, they give identical matrix elements to the ones already listed due to parity invariance in QCD. The short-distance Wilson coefficients $\mathcal{C}_i$ depend on the underlying theory and can be calculated perturbatively. In the Standard Model only matrix elements of $\mathcal{Q}_1^q$ contribute to Δm_q, while all operators do for example for general SUSY extensions of the Standard Model [53]. The matrix elements or bag parameters for the non-SM operators are also useful to estimate the width difference in the Standard Model, where combinations of matrix elements of $\mathcal{Q}_1^q$, $\mathcal{Q}_2^q$, and $\mathcal{Q}_3^q$ contribute to $\Delta\Gamma_q$ at $\mathcal{O}(1/m_b)$ [54, 55].

In this section we report on results from lattice-QCD calculations for the neutral B-meson mixing parameters $\hat{B}_{B_d}$, $\hat{B}_{B_s}$, $f_{B_d}\sqrt{\hat{B}_{B_d}}$, $f_{B_s}\sqrt{\hat{B}_{B_s}}$ and the $SU(3)$-breaking ratios B_{B_s}/B_{B_d} and ξ defined in Eqs. (163), (164), and (166). The results are summarized in Tabs. 34 and 35 and in Figs. 22 and 23. Additional details about the underlying simulations and systematic error estimates are given in Appendix B.6.2. Some collaborations do not provide the RGI quantities $\hat{B}_{B_q}$ but quote instead $B_B(\mu)^{\overline{MS},NDR}$. In such cases we convert the results to the RGI quantities quoted in Tab. 34 using Eq. (164). More details on the conversion factors are provided below in the descriptions of the individual results. We do not provide the B-meson matrix elements of the other operators $\mathcal{Q}_{2-5}$ in this report. They have been calculated in Ref. [9] for the $N_f = 2$ case and in Refs. [56, 57] for $N_f = 2+1$.

There are no new results for $N_f = 2$ reported after the previous FLAG review. However the paper by the ETM collaboration (ETM 13B) [9], which was a preprint, has been published in a journal, thus, it is now eligible to enter the averages. Because this is the only result that passes the quality criteria for $N_f = 2$, we quote their values as our averages in this version:

$$f_{B_d}\sqrt{\hat{B}_{b_d}} = 216(10)\ \text{MeV} \qquad f_{B_s}\sqrt{\hat{B}_{B_s}} = 262(10)\ \text{MeV} \qquad \text{Ref. [9]}, \tag{169}$$
$$N_f = 2: \qquad \hat{B}_{B_d} = 1.30(6) \qquad \hat{B}_{B_s} = 1.32(5) \qquad \text{Ref. [9]}, \tag{170}$$
$$\xi = 1.225(31) \qquad B_{B_s}/B_{B_d} = 1.007(21) \qquad \text{Ref. [9]}. \tag{171}$$

For the $N_f = 2+1$ case there is a new report (RBC/UKQCD 14A) [15] by the RBC/UKQCD collaboration on the neutral B-meson mixing parameter, using domain-wall fermions for the light quarks and the static approximation for the b quark. Used gauge configuration ensembles are the $N_f = 2+1$ domain-wall fermion and Iwasaki gauge actions with two lattice spacings

Collaboration	Ref.	N_f	publication status	continuum extrapolation	chiral extrapolation	finite volume	renormalization/matching	heavy-quark treatment	$f_{\rm B_d}\sqrt{\hat{B}_{\rm B_d}}$	$f_{\rm B_s}\sqrt{\hat{B}_{\rm B_s}}$	$\hat{B}_{\rm B_d}$	$\hat{B}_{\rm B_s}$
FNAL/MILC 16	[57]	2+1	A	★	○	★	○	✓	227.7(9.5)	274.6(8.4)	1.38(12)(6)$^{\odot}$	1.443(88)(48)$^{\odot}$
RBC/UKQCD 14A	[15]	2+1	A	○	○	○	○	✓	240(15)(33)	290(09)(40)	1.17(11)(24)	1.22(06)(19)
FNAL/MILC 11A	[56]	2+1	C	★	○	★	○	✓	250(23)†	291(18)†	–	–
HPQCD 09	[19]	2+1	A	○	○$^{\nabla}$	○	○	✓	216(15)*	266(18)*	1.27(10)*	1.33(6)*
HPQCD 06A	[58]	2+1	A	■	■	★	○	✓	–	281(21)	–	1.17(17)
ETM 13B	[9]	2	A	★	○	○	★	✓	216(6)(8)	262(6)(8)	1.30(5)(3)	1.32(5)(2)
ETM 12A, 12B	[24, 59]	2	C	★	○	○	★	✓	–	–	1.32(8)$^{\diamond}$	1.36(8)$^{\diamond}$

$^{\odot}$ PDG averages of decay constant f_{B^0} and f_{B_s} [2] are used to obtain these values.
† Reported $f_B^2 B$ at $\mu = m_b$ is converted to RGI by multiplying the 2-loop factor 1.517.
$^{\nabla}$ Wrong-spin contributions are not included in the rSχPT fits.
* This result uses an old determination of $r_1 = 0.321(5)$ fm from Ref. [28] that has since been superseded.
$^{\diamond}$ Reported B at $\mu = m_b = 4.35$ GeV is converted to RGI by multiplying the 2-loop factor 1.521.

Table 34: Neutral B- and B_s-meson mixing matrix elements (in MeV) and bag parameters.

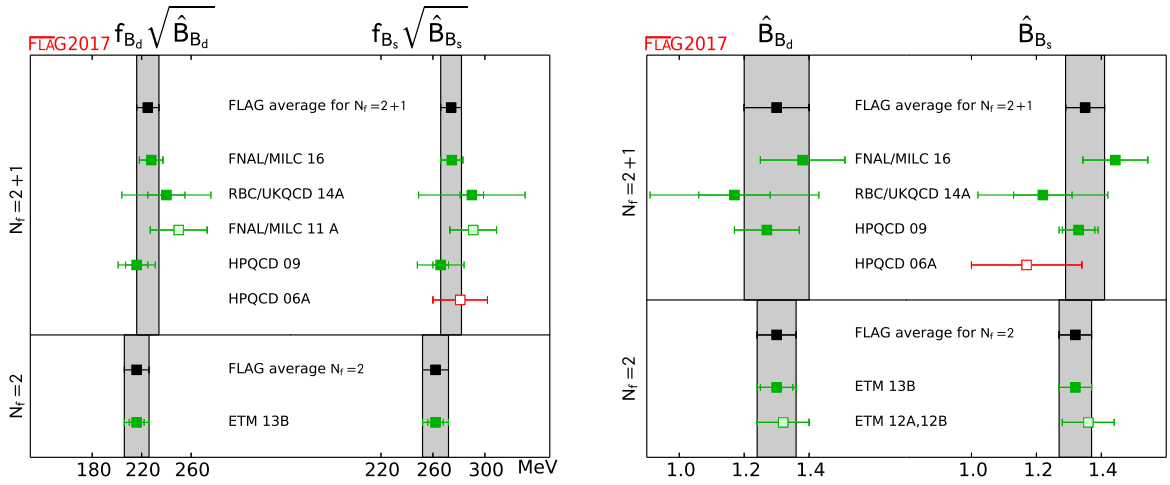

Figure 22: Neutral B- and B_s-meson mixing matrix elements and bag parameters [values in Tab. 34 and Eqs. (169), (172), (170), (173)].

($a \approx 0.09, 0.11$ fm) and a minimum pion mass of about 290 MeV. Two different static-quark actions, smeared with HYP1 [47] and HYP2 [61] are used to further constrain the continuum limit. The operators used are 1-loop $\mathcal{O}(a)$-improved with the tadpole improved perturbation theory. Two different types of chiral formulae are adopted for the combined continuum and

Collaboration	Ref.	N_f	publication status	continuum extrapolation	chiral extrapolation	finite volume	renormalization/matching	heavy-quark treatment	ξ	$B_{\mathrm{B_s}}/B_{\mathrm{B_d}}$
FNAL/MILC 16	[57]	2+1	A	★	○	★	○	✓	1.206(18)	1.033(31)(26)$^{\odot}$
RBC/UKQCD 14A	[15]	2+1	A	○	○	○	○	✓	1.208(41)(52)	1.028(60)(49)
FNAL/MILC 12	[60]	2+1	A	○	○	★	○	✓	1.268(63)	1.06(11)
RBC/UKQCD 10C	[29]	2+1	A	■	■	■	○	✓	1.13(12)	–
HPQCD 09	[19]	2+1	A	○	○$^{\nabla}$	○	○	✓	1.258(33)	1.05(7)
ETM 13B	[9]	2	A	★	○	○	★	✓	1.225(16)(14)(22)	1.007(15)(14)
ETM 12A, 12B	[24, 59]	2	C	★	○	○	★	✓	1.21(6)	1.03(2)

$^{\odot}$ PDG average of the ratio of decay constants f_{B_s}/f_{B^0} [2] is used to obtain the value.
$^{\nabla}$ Wrong-spin contributions are not included in the rSχPT fits.

Table 35: Results for $SU(3)$-breaking ratios of neutral B_d- and B_s-meson mixing matrix elements and bag parameters.

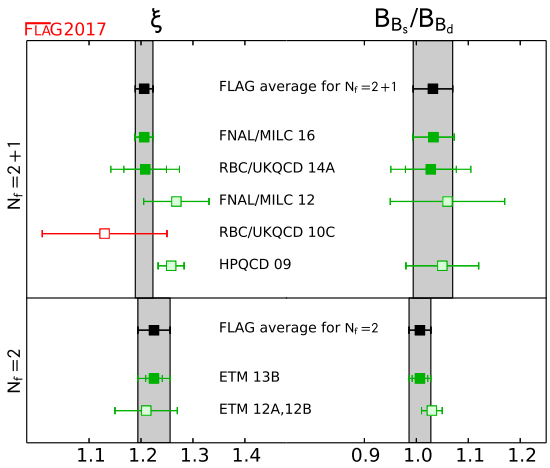

Figure 23: The $SU(3)$-breaking quantities ξ and B_{B_s}/B_{B_d} [values in Tab. 35 and Eqs. (171), (174)].

chiral extrapolation: $SU(2)$ NLO HMχPT and first order polynomial in quark masses with linear $\mathcal{O}(a^2)$ terms. The central values are determined as the average of the results with two different chiral formulae. The systematic error is estimated as half of the full difference of the two, with an exception for the quantity only involving B_s^0, where the NLO χPT is identical

to the first order polynomial. In such cases, the fit excluding the heaviest ud mass point is used for the estimate of the systematic error. The systematic error due to the static approximation is estimated by the simple power counting: the size of Λ_{QCD}/m_b, where $\Lambda_{QCD} = 0.5$ GeV and $m_b(\mu = m_b)^{\overline{\rm MS}} = 4.18$ GeV (PDG) leads to 12%. This is the dominant systematic error for individual $f_B\sqrt{B_B}$ or B_B. Due to this large error, the effect of the inclusion in the FLAG averages of these quantities is small. The dominant systematic error for the $SU(3)$-breaking error, instead, comes from the combined continuum and chiral extrapolation, while the statistical uncertainty is a bit larger than that.

The FNAL/MILC collaboration reported their new results on the neutral B-meson mixing parameters. As the paper [57] appeared after the closing date of FLAG2016, the results had not been taken into our average. Their estimate of the $B^0 - \overline{B^0}$ mixing matrix elements are far improved compared to their older ones as well as all the prior $N_f = 2 + 1$ results. Hence, including the new FNAL/MILC results makes our averages much more precise. The study uses the asqtad action for light quarks and the Fermilab action for the b quark. They used MILC asqtad ensembles spanning four lattice spacings in the range $a \approx 0.045 - 0.12$ fm and RMS pion mass of 257 MeV as the lightest. The lightest Goldstone pion of 177 MeV, at which the RMS mass is 280 MeV, helps constraining the combined chiral and continuum limit analysis with the HMrSχPT to NLO with NNLO analytic terms using a Bayesian analysis. The extension to the finer lattice spacing and closer to physical pion masses together with the quadrupled statistics of the ensembles compared with those used in the earlier studies, as well as the inclusion of the wrong spin contribution [62] which is a staggered fermion artifact, made it possible to achieve the large improvement of the overall precision. Although for each parameter only one lattice volume is available, the finite volume effects are well controlled by using a large enough lattice ($m_\pi^{\rm RMS} L \gtrsim 5$) for all the ensembles. The operator renormalization is done by one-loop lattice perturbation theory with the help of the mostly non-perturbative renormalization method where the quark wave function renormalization is treated non-perturbatively. Let us note that in the report [57] not only the SM $B^0 - \overline{B^0}$ mixing matrix element, but also those with all possible four-quark operators are included. The correlation among the different matrix elements are given, which helps to properly assess the error propagation to phenomenological analyses where combinations of the different matrix elements enter. The authors estimated the effect of omitting the charm quark dynamics. We did not propagate that error to our average. It should also be noted that their main new results are for the $B^0 - \overline{B^0}$ mixing matrix elements, that are $f_{B_d}\sqrt{B_{B_d}}$, $f_{B_s}\sqrt{B_{B_s}}$ and the ratio ξ. They reported also on B_{B_d}, B_{B_s} and B_{B_s}/B_{B_d}. However, the B-meson decay constants needed in order to isolate the bag parameters from the four-fermion matrix elements are taken from the PDG [2] averages, which are obtained using a procedure similar to that used by FLAG. They plan to compute the decay constants on the same gauge field ensembles and then complete the bag parameter calculation on their own in the future. As of now, for the bag parameters we need to use the nested averaging scheme, described in Sec. 8.8, to take into account the possible correlations with this new result to the other ones through the averaged decay constants. The detailed procedure to apply the scheme for this particular

case is provided in Sec. 8.2.1. Now our averages for $N_f = 2 + 1$ are:

$$f_{B_d}\sqrt{\hat{B}_{B_d}} = 225(9)\,\text{MeV} \qquad f_{B_s}\sqrt{\hat{B}_{B_s}} = 274(8)\,\text{MeV} \qquad \text{Refs. [15, 19, 57]}, \tag{172}$$

$$N_f = 2 + 1: \qquad \hat{B}_{B_d} = 1.30(10) \qquad \hat{B}_{B_s} = 1.35(6) \qquad \text{Refs. [15, 19, 57]}, \tag{173}$$

$$\xi = 1.206(17) \qquad B_{B_s}/B_{B_d} = 1.032(38) \qquad \text{Refs. [15, 57]}. \tag{174}$$

Here all the above equations have been updated from the paper version of FLAG2016. The new results from FNAL/MILC 16 [57] entered the average for Eqs. (172), (173), and replaced the earlier FNAL/MILC 12 [60] for Eq. (174).

As discussed in detail in the previous FLAG review [11] HPQCD 09 does not include wrong-spin contributions, which are staggered fermion artifacts, to the chiral extrapolation analysis. It is possible that the effect is significant for ξ and B_{B_s}/B_{B_d}, since the chiral extrapolation error is a dominant one for these $SU(3)$ flavour breaking ratios. Indeed, a test done by FNAL/MILC 12 [60] indicates that the omission of the wrong spin contribution in the chiral analysis may be a significant source of error. We therefore took the conservative choice to exclude ξ and B_{B_s}/B_{B_d} by HPQCD 09 from from our average and we follow the same strategy in this report as well.

We note that the above results are all correlated with each other, due to the use of the same gauge field ensembles for different quantities. The results are also correlated with the averages obtained in Sec. 8.1 and shown in Eq. (156), because the calculations of B-meson decay constants and mixing quantities are performed on the same (or on similar) sets of ensembles, and results obtained by a given collaboration use the same actions and setups. These correlations must be considered when using our averages as inputs to UT fits. In the future, as more independent calculations enter the averages, correlations between the lattice-QCD inputs to the UT fit will become less significant.

8.2.1 Error treatment for B meson bag parameters

The nested scheme discussed in Sec. 8.8 is used to obtain averages of B meson bag parameters. The latest FNAL/MILC measurements (FNAL/MILC 16) use B meson decay constants averaged for PDG [2] to isolate the bag parameter from the mixing matrix elements. Having these bag parameter results in among other standard measurements, correlation of the other results to the FNAL/MILC through the PDG average of decay constants exists. Error estimation of the FLAG average takes into account all possible correlations in order not to underestimate the error we quote. In this spirit the correlation of this type also needs to be addressed.

Three measurements contribute to the average of the B_d meson bag parameter B_{B_d}, FNAL/MILC 16, RBC/UKQCD 14A, HPQCD 09. FNAL/MILC 16 uses f_{B^0} of PDG, which is an average of RBC/UKQCD 14, RBC/UKQCD 14A, HPQCD 12/11A, FNAL/MILC 11 in Table 32. [6] B_{B_d} [RBC/UKQCD 14A] has correlation with that of FNAL/MILC 16, through f_B [RBC/UKQCD 14A]. Also some correlation exists through f_B [RBC/UKQCD 14], which uses the same set of gauge filed configurations as B_{B_d} [RBC/UKQCD 14A].

[6] Isospin correction is made except first one before averaging.

In eq. (218) for this particular case, Q_1 is B_{B_d} [FNAL/MILC 16], Y_1 is $f_{B^0}^2 B_{B_d}$ [FNAL/MILC 16], and $\overline{Z}$ is the PDG average of $f_{B^0}^2$. The most non-trivial part of the nested averaging is to construct the restricted errors $\sigma[f_B^2]_{i'\leftrightarrow k}$ (Eq. (225)) and $\sigma[f_B^2]_{i';j'\leftrightarrow k}$ (Eq. (227)), which goes into the final correlation matrix C_{ij} of B_{B_d} through $\sigma_{1;k}$ (Eq. 223). The restricted summation over (α) labeling the origin of errors in this analysis turns out to be either whole error or statistical error only.

For the correlation of f_B and B_{B_d} both with [RBC/UKQCD 14A], not knowing the information of the correlation, we take total errors 100 % correlated. For example, the heavy quark error, which is $O(1/m_b)$ and most dominant, is common for both. For the correlation of f_B [RBC/UKQCD 14] and B_{B_d} [RBC/UKQCD 14A], which uses different heavy quark formulations but based on the same set of gauge field configurations, only the statistical error is taken correlated. In a similar way, correlation between of the other measurements is determined. In principle we take whole error is correlated between f_B and B_{B_d} if the both results are based on the exact same lattice action for light and heavy quarks and are sharing (at least a part of) the gauge field ensemble. Otherwise only statistical error is taken correlated if two measurements share the gauge field ensemble, or no correlation for the rest, which is summarized in Table 36. Also in a similar way, correlations of f_{B_s} and B_{B_s}, f_{B_s}/f_B and B_{B_s}/B_{B_d} are determined, which are also summarized in Table 36.

The necessary information for constructing the second term in the square root of Eq. (223) is so far provided. Let us also summarize the correlation pattern needed to construct the other part of $\sigma_{i;j}$ for the bag parameters for completeness, which is shown in Table 37.

$\sigma[Z]_{i';j'\leftrightarrow k}$ for k =[RBC/UKQCD 14A]

$i' \setminus j'$	RBC/UKQCD 14A	RBC/UKQCD 14
RBC/UKQCD 14A	all	stat
RBC/UKQCD 14	stat	stat

$\sigma[f_B^2]_{i';j'\leftrightarrow k}$ for k =[HPQCD 09]

$i' \setminus j'$	HPQCD 12/11A	FNAL/MILC 11
HPQCD 12/11A	all	stat
FNAL/MILC 11	stat	stat

$\sigma[f_{B_s}^2]_{i';j'\leftrightarrow k}$ for k =[HPQCD 09]

$i' \setminus j'$	HPQCD 12	HPQCD 11A	FNAL/MILC 11
HPQCD 12	all	stat	stat
HPQCD 11A	stat	stat	stat
FNAL/MILC 11	stat	stat	stat

Table 36: Correlated elements of error composition in the summation over (α) for $\sigma[Z]_{i';j'\leftrightarrow k}$ (Eq. (227)) for $Z = f_B^2, f_{B_s}^2, f_{B_s}^2/f_B^2$. The $i' = j'$ elements express $\sigma[Z]_{i'\leftrightarrow k}$ (Eq. (225)). The elements not listed here are all null.

$i \setminus j$	FNAL/MILC 16	RBC/UKQCD 14A	HPQCD 09
FNAL/MILC 16	–	none	stat
RBC/UKQCD 14A	all	–	none
HPQCD 09	all	none	–

Table 37: Correlated elements of error composition in the summation over (α) for $\sigma_{i;j}$ of B_{B_d}, B_{B_s}, B_{B_s}/B_{B_d}. The i =[FNAL/MILC 16] row expresses the correlations in the first term in the square root in Eq. (223). The j =[FNAL/MILC 16] column represents the correlations for Eq. (228). For B_{B_s}/B_{B_d} only upper 2×2 block is relevant.

8.3 Semileptonic form factors for B decays to light flavours

The Standard Model differential rate for the decay $B_{(s)} \to P\ell\nu$ involving a quark-level $b \to u$ transition is given, at leading order in the weak interaction, by a formula identical to the one for D decays in Eq. (134) but with $D \to B_{(s)}$ and the relevant CKM matrix element $|V_{cq}| \to |V_{ub}|$:

$$\frac{d\Gamma(B_{(s)}\to P\ell\nu)}{dq^2} = \frac{G_F^2|V_{ub}|^2}{24\pi^3}\,\frac{(q^2-m_\ell^2)^2\sqrt{E_P^2-m_P^2}}{q^4 m_{B_{(s)}}^2}\left[\left(1+\frac{m_\ell^2}{2q^2}\right) m_{B_{(s)}}^2 (E_P^2-m_P^2)|f_+(q^2)|^2 + \frac{3m_\ell^2}{8q^2}(m_{B_{(s)}}^2-m_P^2)^2|f_0(q^2)|^2\right]. \quad (175)$$

Again, for $\ell = e, \mu$ the contribution from the scalar form factor f_0 can be neglected, and one has a similar expression to Eq. (136), which in principle allows for a direct extraction of $|V_{ub}|$ by matching theoretical predictions to experimental data. However, while for D (or K) decays the entire physical range $0 \le q^2 \le q^2_{\rm max}$ can be covered with moderate momenta accessible to lattice simulations, in $B \to \pi\ell\nu$ decays one has $q^2_{\rm max} \sim 26$ GeV^2 and only part of the full kinematic range is reachable. As a consequence, obtaining $|V_{ub}|$ from $B \to \pi\ell\nu$ is more complicated than obtaining $|V_{cd(s)}|$ from semileptonic D-meson decays.

In practice, lattice computations are restricted to small values of the momentum transfer (see Sec. 7.2) where statistical and momentum-dependent discretization errors can be controlled,[7] which in existing calculations roughly cover the upper third of the kinematically allowed q^2 range. Since, on the other hand, the decay rate is suppressed by phase space at large q^2, most of the semileptonic $B \to \pi$ events are selected in experiment at lower values of q^2, leading to more accurate experimental results for the binned differential rate in that region.[8] It is therefore a challenge to find a window of intermediate values of q^2 at which both the experimental and lattice results can be reliably evaluated.

In current practice, the extraction of CKM matrix elements requires that both experimental and lattice data for the q^2 dependence be parameterized by fitting data to a specific ansatz. Before the generalization of the sophisticated ansätze that will be discussed below, the most common procedure to overcome this difficulty involved matching the theoretical prediction and the experimental result for the integrated decay rate over some finite interval in q^2,

$$\Delta\zeta = \frac{1}{|V_{ub}|^2}\int_{q_1^2}^{q_2^2}\left(\frac{d\Gamma}{dq^2}\right)dq^2\,. \quad (176)$$

In the most recent literature, it has become customary to perform a joint fit to lattice and experimental results, keeping the relative normalization $|V_{ub}|^2$ as a free parameter. In either case, good control of the systematic uncertainty induced by the choice of parameterization is crucial to obtain a precise determination of $|V_{ub}|$.

[7] The variance of hadron correlation functions at nonzero three-momentum is dominated at large Euclidean times by zero-momentum multiparticle states [63]; therefore the noise-to-signal grows more rapidly than for the vanishing three-momentum case.

[8] Upcoming data from Belle II are expected to significantly improve the precision of experimental results, in particular, for larger values of q^2.

8.3.1 Parameterizations of semileptonic form factors

In this section, we discuss the description of the q^2 dependence of form factors, using the vector form factor f_+ of $B \to \pi\ell\nu$ decays as a benchmark case. Since in this channel the parameterization of the q^2 dependence is crucial for the extraction of $|V_{ub}|$ from the existing measurements (involving decays to light leptons), as explained above, it has been studied in great detail in the literature. Some comments about the generalization of the techniques involved will follow.

The vector form factor for $B \to \pi\ell\nu$ All form factors are analytic functions of q^2 outside physical poles and inelastic threshold branch points; in the case of $B \to \pi\ell\nu$, the only pole expected below the $B\pi$ production region, starting at $q^2 = t_+ = (m_B + m_\pi)^2$, is the B^*. A simple ansatz for the q^2 dependence of the $B \to \pi\ell\nu$ semileptonic form factors that incorporates vector-meson dominance is the Bećirević-Kaidalov (BK) parameterization [64], which for the vector form factor reads:

$$f_+(q^2) = \frac{f(0)}{(1-q^2/m_{B^*}^2)(1-\alpha q^2/m_{B^*}^2)} \,. \tag{177}$$

Because the BK ansatz has few free parameters, it has been used extensively to parameterize the shape of experimental branching-fraction measurements and theoretical form-factor calculations. A variant of this parameterization proposed by Ball and Zwicky (BZ) adds extra pole factors to the expressions in Eq. (177) in order to mimic the effect of multiparticle states [65]. A similar idea, extending the use of effective poles also to $D \to \pi\ell\nu$ decays, is explored in Ref. [66]. Finally, yet another variant (RH) has been proposed by Hill in Ref. [67]. Although all of these parameterizations capture some known properties of form factors, they do not manifestly satisfy others. For example, perturbative QCD scaling constrains the behaviour of f_+ in the deep Euclidean region [68–70], and angular momentum conservation constrains the asymptotic behaviour near thresholds — e.g., $\mathrm{Im}\, f_+(q^2) \sim (q^2 - t_+)^{3/2}$ (see, e.g., Ref. [71]). Most importantly, these parameterizations do not allow for an easy quantification of systematic uncertainties.

A more systematic approach that improves upon the use of simple models for the q^2 behaviour exploits the positivity and analyticity properties of two-point functions of vector currents to obtain optimal parameterizations of form factors [70, 72–76]. Any form factor f can be shown to admit a series expansion of the form

$$f(q^2) = \frac{1}{B(q^2)\phi(q^2,t_0)} \sum_{n=0}^{\infty} a_n(t_0)\, z(q^2,t_0)^n \,, \tag{178}$$

where the squared momentum transfer is replaced by the variable

$$z(q^2,t_0) = \frac{\sqrt{t_+-q^2}-\sqrt{t_+-t_0}}{\sqrt{t_+-q^2}+\sqrt{t_+-t_0}} \,. \tag{179}$$

This is a conformal transformation, depending on an arbitrary real parameter $t_0 < t_+$, that maps the q^2 plane cut for $q^2 \geq t_+$ onto the disk $|z(q^2,t_0)| < 1$ in the z complex plane. The function $B(q^2)$ is called the *Blaschke factor*, and contains poles and cuts below t_+ — for instance, in the case of $B \to \pi$ decays,

$$B(q^2) = \frac{z(q^2,t_0)-z(m_{B^*}^2,t_0)}{1-z(q^2,t_0)z(m_{B^*}^2,t_0)} = z(q^2,m_{B^*}^2) \,. \tag{180}$$

Finally, the quantity $\phi(q^2, t_0)$, called the *outer function*, is some otherwise arbitrary function that does not introduce further poles or branch cuts. The crucial property of this series expansion is that the sum of the squares of the coefficients

$$\sum_{n=0}^{\infty} a_n^2 = \tfrac{1}{2\pi i} \oint \tfrac{dz}{z} \, |B(z)\phi(z)f(z)|^2 \,, \tag{181}$$

is a finite quantity. Therefore, by using this parameterization an absolute bound to the uncertainty induced by truncating the series can be obtained. The aim in choosing ϕ is to obtain a bound that is useful in practice, while (ideally) preserving the correct behaviour of the form factor at high q^2 and around thresholds.

The simplest form of the bound would correspond to $\sum_{n=0}^{\infty} a_n^2 = 1$. *Imposing* this bound yields the following "standard" choice for the outer function

$$\begin{aligned} \phi(q^2, t_0) = & \sqrt{\tfrac{1}{32\pi\chi_{1^-}(0)}} \left(\sqrt{t_+ - q^2} + \sqrt{t_+ - t_0}\right) \\ & \times \left(\sqrt{t_+ - q^2} + \sqrt{t_+ - t_-}\right)^{3/2} \left(\sqrt{t_+ - q^2} + \sqrt{t_+}\right)^{-5} \tfrac{t_+ - q^2}{(t_+ - t_0)^{1/4}} \,, \end{aligned} \tag{182}$$

where $t_- = (m_B - m_\pi)^2$, and $\chi_{1^-}(0)$ is the derivative of the transverse component of the polarization function (i.e., the Fourier transform of the vector two-point function) $\Pi_{\mu\nu}(q)$ at Euclidian momentum $Q^2 = -q^2 = 0$. It is computed perturbatively, using operator product expansion techniques, by relating the $B \to \pi\ell\nu$ decay amplitude to $\ell\nu \to B\pi$ inelastic scattering via crossing symmetry and reproducing the correct value of the inclusive $\ell\nu \to X_b$ amplitude. We will refer to the series parameterization with the outer function in Eq. (182) as Boyd, Grinstein, and Lebed (BGL). The perturbative and OPE truncations imply that the bound is not strict, and one should take it as

$$\sum_{n=0}^{N} a_n^2 \lesssim 1 \,, \tag{183}$$

where this holds for any choice of N. Since the values of $|z|$ in the kinematical region of interest are well below 1 for judicious choices of t_0, this provides a very stringent bound on systematic uncertainties related to truncation for $N \geq 2$. On the other hand, the outer function in Eq. (182) is somewhat unwieldy and, more relevantly, spoils the correct large q^2 behaviour and induces an unphysical singularity at the $B\pi$ threshold.

A simpler choice of outer function has been proposed by Bourrely, Caprini and Lellouch (BCL) in Ref. [71], which leads to a parameterization of the form

$$f_+(q^2) = \tfrac{1}{1 - q^2/m_{B^*}^2} \sum_{n=0}^{N} a_n^+(t_0) z(q^2, t_0)^n \,. \tag{184}$$

This satisfies all the basic properties of the form factor, at the price of changing the expression for the bound to

$$\sum_{j,k=0}^{N} B_{jk}(t_0) a_j^+(t_0) a_k^+(t_0) \leq 1 \,. \tag{185}$$

The constants B_{jk} can be computed and shown to be $|B_{jk}| \lesssim \mathcal{O}(10^{-2})$ for judicious choices of t_0; therefore, one again finds that truncating at $N \geq 2$ provides sufficiently stringent bounds for the current level of experimental and theoretical precision. It is actually possible to optimize the properties of the expansion by taking

$$t_0 = t_{\rm opt} = (m_B + m_\pi)(\sqrt{m_B} - \sqrt{m_\pi})^2 \,, \tag{186}$$

which for physical values of the masses results in the semileptonic domain being mapped onto the symmetric interval $|z| \lesssim 0.279$ (where this range differs slightly for the $B^\pm$ and B^0 decay channels), minimizing the maximum truncation error. If one also imposes that the asymptotic behaviour $\mathrm{Im}\, f_+(q^2) \sim (q^2 - t_+)^{3/2}$ near threshold is satisfied, then the highest-order coefficient is further constrained as

$$a_N^+ = -\tfrac{(-1)^N}{N} \sum_{n=0}^{N-1} (-1)^n \, n \, a_n^+ \,. \tag{187}$$

Substituting the above constraint on a_N^+ into Eq. (184) leads to the constrained BCL parameterization

$$f_+(q^2) = \tfrac{1}{1-q^2/m_{B^*}^2} \sum_{n=0}^{N-1} a_n^+ \left[z^n - (-1)^{n-N} \, \tfrac{n}{N} \, z^N \right] \,, \tag{188}$$

which is the standard implementation of the BCL parameterization used in the literature.

Parameterizations of the BGL and BCL kind, to which we will refer collectively as "z-parameterizations", have already been adopted by the BaBar and Belle collaborations to report their results, and also by the Heavy Flavour Averaging Group (HFAG). Some lattice collaborations, such as FNAL/MILC and ALPHA, have already started to report their results for form factors in this way. The emerging trend is to use the BCL parameterization as a standard way of presenting results for the q^2 dependence of semileptonic form factors. Our policy will be to quote results for z-parameterizations when the latter are provided in the paper (including the covariance matrix of the fits); when this is not the case, but the published form factors include the full correlation matrix for values at different q^2, we will perform our own fit to the constrained BCL ansatz in Eq. (188); otherwise no fit will be quoted. We however stress the importance of providing, apart from parameterization coefficients, values for the form factors themselves (in the continuum limit and at physical quark masses) for a number of values of q^2, so that the results can be independently parameterized by the readers if so wished.

The scalar form factor for $B \to \pi\ell\nu$ The discussion of scalar $B \to \pi$ form factor is very similar. The main differences are the absence of a constraint analogue to Eq. (187) and the choice of the overall pole function. In our fits we adopt the simple expansion:

$$f_0(q^2) = \sum_{n=0}^{N-1} a_n^0 \, z^n \,. \tag{189}$$

We do impose the exact kinematical constraint $f_+(0) = f_0(0)$ by expressing the a_{N-1}^0 coefficient in terms of all remaining a_n^+ and a_n^0 coefficients. This constraint introduces important

correlations between the a_n^+ and a_n^0 coefficients; thus only lattice calculations that present the correlations between the vector and scalar form factors can be used in an average that takes into account the constraint at $q^2 = 0$.

Finally we point out that we do not need to use the same number of parameters for the vector and scalar form factors. For instance, with $(N^+ = 3, N^0 = 3)$ we have $a^+_{0,1,2}$ and $a^0_{0,1}$, while with $(N^+ = 3, N^0 = 4)$ we have $a^+_{0,1,2}$ and $a^0_{0,1,2}$ as independent fit parameters. In our average we will choose the combination that optimizes uncertainties.

Extension to other form factors The discussion above largely extends to form factors for other semileptonic transitions (e.g., $B_s \to K$ and $B_{(s)} \to D^{(*)}_{(s)}$, and semileptonic D and K decays). As a matter of fact, after the publication of our previous review z-parameterizations have been applied in several such cases, as discussed in the relevant sections.

A general discussion of semileptonic meson decay in this context can be found, e.g., in Ref. [77]. Extending what has been discussed above for $B \to \pi$, the form factors for a generic $H \to L$ transition will display a cut starting at the production threshold t_+, and the optimal value of t_0 required in z-parameterizations is $t_0 = t_+(1 - \sqrt{1 - t_-/t_+})$ (where $t_\pm = (m_H \pm m_L)^2$). For unitarity bounds to apply, the Blaschke factor has to include all sub-threshold poles with the quantum numbers of the hadronic current — i.e., vector (resp. scalar) resonances in $B\pi$ scattering for the vector (resp. scalar) form factors of $B \to \pi$, $B_s \to K$, or $\Lambda_b \to p$; and vector (resp. scalar) resonances in $B_c\pi$ scattering for the vector (resp. scalar) form factors of $B \to D$ or $\Lambda_b \to \Lambda_c$.[9] Thus, as emphasized above, the control over systematic uncertainties brought in by using z-parameterizations strongly depends on implementation details. This has practical consequences, in particular, when the resonance spectrum in a given channel is not sufficiently well-known. Caveats may also apply for channels where resonances with a nonnegligible width appear. A further issue is whether $t_+ = (m_H + m_L)^2$ is the proper choice for the start of the cut in cases such as $B_s \to K\ell\nu$ and $B \to D\ell\nu$, where there are lighter two-particle states that project on the current (B,π and B_c,π for the two processes, respectively).[10] In any such situation, it is not clear a priori that a given z-parameterization will satisfy strict bounds, as has been seen, e.g., in determinations of the proton charge radius from electron-proton scattering [78–80].

The HPQCD Collaboration pioneered a variation on the z-parameterization approach, which they refer to as a "modified z-expansion," that is used to simultaneously extrapolate their lattice simulation data to the physical light-quark masses and the continuum limit, and to interpolate/extrapolate their lattice data in q^2. This entails allowing the coefficients a_n to depend on the light-quark masses, squared lattice spacing, and, in some cases the charm-quark mass and pion or kaon energy. Because the modified z-expansion is not derived from an underlying effective field theory, there are several potential concerns with this approach that have yet to be studied. The most significant is that there is no theoretical derivation relating the coefficients of the modified z-expansion to those of the physical coefficients measured in experiment; it therefore introduces an unquantified model dependence in the form-factor shape. As a result, the applicability of unitarity bounds has to be examined carefully. Related to this, z-parameterization coefficients implicitly depend on quark masses, and particular care

[9] A more complicated analytic structure may arise in other cases, such as channels with vector mesons in the final state. We will however not discuss form-factor parameterizations for any such process.

[10] We are grateful to G. Herdoíza, R.J. Hill, A. Kronfeld and A. Szczepaniak for illuminating discussions on this issue.

should be taken in the event that some state can move across the inelastic threshold as quark masses are changed (which would in turn also affect the form of the Blaschke factor). Also, the lattice spacing dependence of form factors provided by Symanzik effective theory techniques may not extend trivially to z-parameterization coefficients. The modified z-expansion is now being utilized by collaborations other than HPQCD and for quantities other than $D \to \pi\ell\nu$ and $D \to K\ell\nu$, where it was originally employed. We advise treating results that utilize the modified z-expansion to obtain form-factor shapes and CKM matrix elements with caution, however, since the systematics of this approach warrant further study.

8.3.2 Form factors for $B \to \pi\ell\nu$

The semileptonic decay processes $B \to \pi\ell\nu$ enable determinations of the CKM matrixelement $|V_{ub}|$ within the Standard Model via Eq. (175). At the time of our previous review, the only available results for $B \to \pi\ell\nu$ form factors came from the HPQCD [81] and FNAL/MILC [82] Collaborations. Only HPQCD provided results for the scalar form factor f_0. The last two years, however, have witnessed significant progress: FNAL/MILC have significantly upgraded their $B \to \pi\ell\nu$ results [83],[11] while a completely new computation has been provided by RBC/UKQCD [84]. All the above computations employ $N_f = 2+1$ dynamical configurations, and provide values for both form factors f_+ and f_0. Finally, HPQCD have recently published the first $N_f = 2+1+1$ results for the $B \to \pi\ell\nu$ scalar form factor, working at zero recoil and pion masses down to the physical value [85]; this adds to previous reports on ongoing work to upgrade their 2006 computation [86, 87]. Since this latter result has no immediate impact on current $|V_{ub}|$ determinations, which come from the vector-form-factor-dominated decay channels into light leptons, we will from now on concentrate on the $N_f = 2+1$ determinations of the q^2 dependence of $B \to \pi$ form factors.

Both the HPQCD and the FNAL/MILC computations of $B \to \pi\ell\nu$ amplitudes use ensembles of gauge configurations with $N_f = 2+1$ flavours of rooted staggered quarks produced by the MILC Collaboration; however, the latest FNAL/MILC work makes a much more extensive use of the currently available ensembles, both in terms of lattice spacings and light-quark masses. HPQCD have results at two values of the lattice spacing ($a \sim 0.12,\ 0.09$ fm), while FNAL/MILC employs four values ($a \sim 0.12,\ 0.09,\ 0.06,\ 0.045$ fm). Lattice-discretization effects are estimated within HMrSχPT in the FNAL/MILC computation, while HPQCD quotes the results at $a \sim 0.12$ fm as central values and uses the $a \sim 0.09$ fm results to quote an uncertainty. The relative scale is fixed in both cases through r_1/a. HPQCD set the absolute scale through the Υ $2S$–$1S$ splitting, while FNAL/MILC uses a combination of f_π and the same Υ splitting, as described in Ref. [18]. The spatial extent of the lattices employed by HPQCD is $L \simeq 2.4$ fm, save for the lightest mass point (at $a \sim 0.09$ fm) for which $L \simeq 2.9$ fm. FNAL/MILC, on the other hand, uses extents up to $L \simeq 5.8$ fm, in order to allow for light pion masses while keeping finite volume effects under control. Indeed, while in the 2006 HPQCD work the lightest RMS pion mass is 400 MeV, the latest FNAL/MILC work includes pions as light as 165 MeV — in both cases the bound $m_\pi L \gtrsim 3.8$ is kept. Other than the qualitatively different range of MILC ensembles used in the two computations, the main difference between HPQCD and FNAL/MILC lies in the treatment of heavy quarks. HPQCD uses the NRQCD formalism, with a 1-loop matching of the relevant currents to the ones in the relativistic theory. FNAL/MILC employs the clover action with the Fermilab in-

[11] Since the new FNAL/MILC results supersede Ref. [82], we will not discuss this latter work in the present version of the review.

terpretation, with a mostly nonperturbative renormalization of the relevant currents, within which light-light and heavy-heavy currents are renormalized nonperturbatively and 1-loop perturbation theory is used for the relative normalization. (See Tab. 38; full details about the computations are provided in tables in Appendix B.6.3.)

The RBC/UKQCD computation is based on $N_f = 2 + 1$ DWF ensembles at two values of the lattice spacing ($a \sim 0.12,\ 0.09$ fm), and pion masses in a narrow interval ranging from slightly above 400 MeV to slightly below 300 MeV, keeping $m_\pi L \gtrsim 4$. The scale is set using the Ω^- baryon mass. Discretization effects coming from the light sector are estimated in the 1% ballpark using HMχPT supplemented with effective higher-order interactions to describe cutoff effects. The b quark is treated using the Columbia RHQ action, with a mostly nonperturbative renormalization of the relevant currents. Discretization effects coming from the heavy sector are estimated with power-counting arguments to be below 2%.

Given the large kinematical range available in the $B \to \pi$ transition, chiral extrapolations are an important source of systematic uncertainty: apart from the eventual need to reach physical pion masses in the extrapolation, the applicability of χPT is not guaranteed for large values of the pion energy E_π. Indeed, in all computations E_π reaches values in the 1 GeV ballpark, and chiral extrapolation systematics is the dominant source of errors. FNAL/MILC uses $SU(2)$ NLO HMrSχPT for the continuum-chiral extrapolation, supplemented by NNLO analytic terms and hard-pion χPT terms [88];[12] systematic uncertainties are estimated through an extensive study of the effects of varying the specific fit ansatz and/or data range. RBC/UKQCD uses $SU(2)$ hard-pion HMχPT to perform its combined continuum-chiral extrapolation, and obtains sizeable estimates for systematic uncertainties by varying the ansätze and ranges used in fits. HPQCD performs chiral extrapolations using HMrSχPT formulae, and estimates systematic uncertainties by comparing the result with the ones from fits to a linear behaviour in the light-quark mass, continuum HMχPT, and partially quenched HMrSχPT formulae (including also data with different sea and valence light-quark masses).

FNAL/MILC and RBC/UKQCD describe the q^2 dependence of f_+ and f_0 by applying a BCL parameterization to the form factors extrapolated to the continuum limit, within the range of values of q^2 covered by data. RBC/UKQCD generate synthetic data for the form factors at some values of q^2 (evenly spaced in z) from the continuous function of q^2 obtained from the joint chiral-continuum extrapolation, which are then used as input for the fits. After having checked that the kinematical constraint $f_+(0) = f_0(0)$ is satisfied within errors by the extrapolation to $q^2 = 0$ of the results of separate fits, this constraint is imposed to improve fit quality. In the case of FNAL/MILC, rather than producing synthetic data a functional method is used to extract the z-parameterization directly from the fit functions employed in the continuum-chiral extrapolation. The resulting preferred fits for both works are quoted in Tab. 38. In the case of HPQCD, the parameterization of the q^2 dependence of form factors is somewhat intertwined with chiral extrapolations: a set of fiducial values $\{E_\pi^{(n)}\}$ is fixed for each value of the light-quark mass, and $f_{+,0}$ are interpolated to each of the $E_\pi^{(n)}$; chiral extrapolations are then performed at fixed E_π (i.e. m_π and q^2 are varied subject to E_π=constant). The interpolation is performed using a BZ ansatz. The q^2 dependence of the resulting form factors in the chiral limit is then described by means of a BZ ansatz, which is cross-checked against BK, RH, and BGL parameterizations. Unfortunately, the correlation matrix for the values of the form factors at different q^2 is not provided, which severely limits

[12] Note that issues are known to exist with hard-pion χPT, cf. Ref. [89].

Collaboration	Ref.	N_f	publication status	continuum extrapolation	chiral extrapolation	finite volume	renormalization	heavy-quark treatment	z-parameterization	$\Delta\zeta^{B\pi}$
FNAL/MILC 15	[83]	2+1	A	★	○	★	○	✓	BCL	n/a
RBC/UKQCD 15	[84]	2+1	A	○	○	○	○	✓	BCL	1.77(34)
HPQCD 06	[81]	2+1	A	○	○	○	○	✓	n/a	2.07(41)(39)

Table 38: Results for the $B \to \pi\ell\nu$ semileptonic form factor. The quantity $\Delta\zeta$ is defined in Eq. (176); the quoted values correspond to $q_1 = 4$ GeV, $q_2 = q_{max}$, and are given in ps^{-1}.

the possibilities of combining them with other computations into a global z-parameterization.

Based on the parameterized form factors, HPQCD and RBC/UKQCD provide values for integrated decay rates $\Delta\zeta^{B\pi}$, as defined in Eq. (176); they are quoted in Tab. 38. The latest FNAL/MILC work, on the other hand, does not quote a value for the integrated ratio. Furthermore, as mentioned above, the field has recently moved forward to determine CKM matrix elements from direct joint fits of experimental results and theoretical form factors, rather than a matching through $\Delta\zeta^{B\pi}$. Thus, we will not provide here a FLAG average for the integrated rate, and focus on averaging lattice results for the form factors themselves.

In our previous review, we averaged the results for $f_+(q^2)$ in HPQCD 06 and the superseded FNAL/MILC 2008 determination [82], fitting them jointly to our preferred BCL z-parameterization, Eq. (188). The new results do not, however, allow for an update of such a joint fit: RBC/UKQCD only provides synthetic values of f_+ and f_0 at a few values of q^2 as an illustration of their results, and FNAL/MILC does not quote synthetic values at all. In both cases, full results for BCL z-parameterizations defined by Eq. (188) are quoted. In the case of HPQCD 06, unfortunately, a fit to a BCL z-parameterization is not possible, as discussed above.

In order to combine these form factor calculations we start from sets of synthetic data for several q^2 values. HPQCD and RBC/UKQCD provide directly this information; FNAL/MILC presents only fits to a BCL z-parametrization from which we can easily generate an equivalent set of form factor values. It is important to note that in both the RBC/UKQCD synthetic data and the FNAL/MILC z-parametrization fits the kinematic constraint at $q^2 = 0$ is automatically included (in the FNAL/MILC case the constraint is manifest in an exact degeneracy of the (a_n^+, a_n^0) covariance matrix). Due to these considerations, in our opinion the most accurate procedure is to perform a simultaneous fit to all synthetic data for the vector and scalar form factors. Unfortunately the absence of information on the correlation in the HPQCD result between the vector and scalar form factors even at a single q^2 point makes it impossible to include consistently this calculation in the overall fit. In fact, the HPQCD and FNAL/MILC statistical uncertainties are highly correlated (because they are based on overalapping subsets of MILC $N_f = 2 + 1$ ensembles) and, without knowledge of the $f_+ - f_0$ correlation we are

unable to construct the HPQCD-FNAL/MILC off-diagonal entries of the overall covariance matrix.

In conclusion, we will present as our best result a combined vector and scalar form factor fit to the FNAL/MILC and RBC/UKQCD results that we treat as completely uncorrelated. For sake of completeness we will also show the results of a vector form factor fit alone in which we include one HPQCD datum at $q^2 = 17.34$ GeV^2 assuming conservatively a 100% correlation between the statistical error of this point and of all FNAL/MILC synthetic data. In spite of contributing just one point, the HPQCD datum has a significant weight in the fit due to its small overall uncertainty. We stress again that this procedure is slightly inconsistent because FNAL/MILC and RBC/UKQCD include information on the kinematic constraint at $q^2 = 0$ in their f_+ results.

The resulting dataset is then fitted to the BCL parameterization in Eqs. (188) and (189). We assess the systematic uncertainty due to truncating the series expansion by considering fits to different orders in z. In the two panels of Fig. 24 we show the FNAL/MILC, RBC/UKQCD, and HPQCD data points for $(1 - q^2/m^2_{B^*})f_+(q^2)$ and $f_0(q^2)$ versus z. The data is highly linear and we get a good χ^2/d.o.f. with $N^+ = N^0 = 3$. Note that this implies three independent parameters for f_+ corresponding to a polynomial through $\mathcal{O}(z^3)$ and two independent parameters for f_0 corresponding to a polynomial through $\mathcal{O}(z^2)$ (the coefficient a^0_2 is fixed using the $q^2 = 0$ kinematic constraint). We cannot constrain the coefficients of the z-expansion beyond this order; for instance, including a fourth parameter in f_+ yields to 100% uncertainties on a^+_2 and a^+_3. The outcome of the five-parameter BCL fit to the FNAL/MILC and RBC/UKQCD calculations is:

$B \to \pi$ ($N_f = 2 + 1$)

	Central Values	Correlation Matrix				
a^+_0	0.404 (13)	1	0.404	0.118	0.327	0.344
a^+_1	-0.68 (13)	0.404	1	0.741	0.310	0.900
a^+_2	-0.86 (61)	0.118	0.741	1	0.363	0.886
a^0_0	0.490 (21)	0.327	0.310	0.363	1	0.233
a^0_1	-1.61 (16)	0.344	0.900	0.886	0.233	1

The uncertainties on $a^{+,0}_0$, $a^{+,0}_1$ and a^+_2 encompass the central values obtained from $N^+ = 2, 4$ and $N^0 = 2, 4, 5$ fits and thus adequately reflect the systematic uncertainty on those series coefficients. This can be used as the averaged FLAG result for the lattice-computed form factor $f_+(q^2)$. The coefficient a^+_3 can be obtained from the values for a^+_0–a^+_2 using Eq. (187). The coefficient a^0_3 can be obtained from all other coefficients imposing the $f_+(q^2 = 0) = f_0(q^2 = 0)$ constraint. The fit is illustrated in Fig. 24.

It is worth stressing that, with respect to our average in the previous edition of the FLAG report, the relative error on a^+_0, which dominates the theory contribution to the determination of $|V_{ub}|$, has decreased from 7.3% to 3.2%. The dominant factor in this remarkable improvement is the new FNAL/MILC determination of f_+. We emphasize that future lattice-QCD calculations of semileptonic form factors should publish their full statistical and systematic correlation matrices to enable others to use the data. It is also preferable to present a set of synthetic form factors data equivalent to the z-fit results, since this allows for an independent analysis that avoids further assumptions about the compatibility of the procedures to

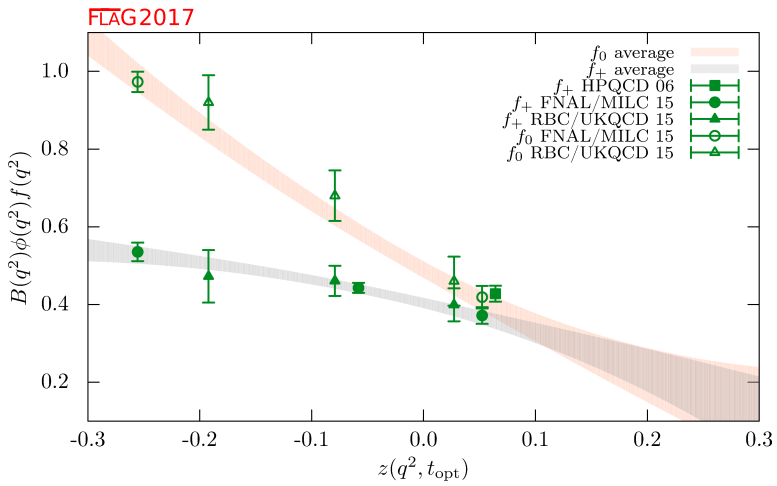

Figure 24: The form factors $(1 - q^2/m_{B^*}^2)f_+(q^2)$ and $f_0(q^2)$ for $B \to \pi\ell\nu$ plotted versus z. (See text for a discussion of the dataset.) The grey and orange bands display our preferred $N^+ = N^0 = 3$ BCL fit (five parameters) to the plotted data with errors.

arrive at a given z-parameterization.[13] It is also preferable to present covariance/correlation matrices with enough significant digits to calculate correctly all their eigenvalues.

For the sake of completeness, we present also a standalone z-fit to the vector form factor alone. In this fit we are able to include the single f_+ point at $q^2 = 17.34$ GeV^2 that we mentioned above. This fit uses the FNAL/MILC and RBC/UKQCD results that do make use of the kinematic constraint at $q^2 = 0$ but is otherwise unbiased. The results of the three-parameter BCL fit to the HPQCD, FNAL/MILC and RBC/UKQCD calculations of the vector form factor are:

$$N_f = 2+1: \qquad a_0^+ = 0.421(13)\,, \qquad a_1^+ = -0.35(10)\,, \qquad a_2^+ = -0.41(64)\,; \tag{190}$$

$$\mathrm{corr}(a_i, a_j) = \begin{pmatrix} 1.000 & 0.306 & 0.084 \\ 0.306 & 1.000 & 0.856 \\ 0.084 & 0.856 & 1.000 \end{pmatrix}.$$

Note that the a_0^+ coefficient, that is the most relevant for input to the extraction of V_{ub} from semileptonic $B \to \pi\ell\nu_\ell (\ell = e, \mu)$ decays, shifts by about a standard deviation.

8.3.3 Form factors for $B_s \to K\ell\nu$

Similar to $B \to \pi\ell\nu$, measurements of $B_s \to K\ell\nu$ enable determinations of the CKM matrix element $|V_{ub}|$ within the Standard Model via Eq. (175). From the lattice point of view the two channels are very similar — as a matter of fact, $B_s \to K\ell\nu$ is actually somewhat simpler, in that the fact that the kaon mass region is easily accessed by all simulations makes the systematic uncertainties related to chiral extrapolation smaller. On the other hand, $B_s \to K\ell\nu$ channels have not been measured experimentally yet, and therefore lattice results provide SM predictions for the relevant rates.

[13] Note that generating synthetic data is a trivial task but less so the number of required points and the q^2 values that lead to an optimal description of the form factors.

Collaboration	Ref.	N_f	publication status	continuum extrapolation	chiral extrapolation	finite volume	renormalization	heavy-quark treatment	z-parameterization
RBC/UKQCD 15	[84]	2+1	A	○	○	○	○	✓	BCL
HPQCD 14	[90]	2+1	A	○	○	○	○	✓	BCL†

† Results from modified z-expansion.

Table 39: Results for the $B_s \to K\ell\nu$ semileptonic form factor.

At the time of our previous review, only preliminary results existed for $B_s \to K\ell\nu$ form factors. However, as with $B \to \pi\ell\nu$, great progress has been made during the last year, and first full results for $B_s \to K\ell\nu$ form factors have been provided by HPQCD [90] and RBC/UKQCD [83] for both form factors f_+ and f_0, in both cases using $N_f = 2+1$ dynamical configurations. Finally, the ALPHA Collaboration determination of $B_s \to K\ell\nu$ form factors with $N_f = 2$ is also well underway [91]; however, since the latter is so far described only in conference proceedings which do not provide quotable results, it will not be discussed here.

The RBC/UKQCD computation has been published together with the $B \to \pi\ell\nu$ computation discussed in Sec. 8.3.2, all technical details being practically identical. The main difference is that errors are significantly smaller, mostly due to the reduction of systematic uncertainties due to the chiral extrapolation; detailed information is provided in tables in Appendix B.6.3. The HPQCD computation uses ensembles of gauge configurations with $N_f = 2 + 1$ flavours of rooted staggered quarks produced by the MILC Collaboration at two values of the lattice spacing ($a \sim 0.12,\ 0.09$ fm), for three and two different sea-pion masses, respectively, down to a value of 260 MeV. The b quark is treated within the NRQCD formalism, with a 1-loop matching of the relevant currents to the ones in the relativistic theory, omitting terms of $\mathcal{O}(\alpha_s\Lambda_{\rm QCD}/m_b)$. A HISQ action is used for the valence s quark. The continuum-chiral extrapolation is combined with the description of the q^2 dependence of the form factors into a modified z-expansion (cf. Sec. 8.3.1) that formally coincides in the continuum with the BCL ansatz. The dependence of form factors on the pion energy and quark masses is fitted to a 1-loop ansatz inspired by hard-pion χPT [88], that factorizes out the chiral logarithms describing soft physics. See Tab. 39 and the tables in Appendix B.6.3 for full details.

Both RBC/UKQCD and HPQCD quote values for integrated differential decay rates over the full kinematically available region. However, since the absence of experiment makes the relevant integration interval subject to change, we will not discuss them here, and focus on averages of form factors. In order to proceed to combine the results from the two collaborations, we will follow a similar approach to the one adopted above for $B \to \pi\ell\nu$: we will take as direct input the synthetic values of the form factors provided by RBC/UKQCD, use the preferred HPQCD parameterization to produce synthetic values, and perform a joint fit to

the two datasets.

Note that the kinematic constraint at $q^2 = 0$ is included explicitly in the results presented by HPQCD (the coefficient b_0^0 is expressed analytically in terms of all others) and implicitly in the synthetic data provided by RBC/UKQCD. Therefore, following the procedure we adopted for the $B \to \pi$ case, we present a joint fit to the vector and scalar form factors and implement explicitly the $q^2 = 0$ constraint by expressing the coefficient $b^0_{N^0-1}$ in terms of all others.

For the fits we employ a BCL ansatz with $t_+ = (M_{B_s} + M_{K^\pm})^2 \simeq 34.35$ GeV^2 and $t_0 = (M_{B_s} + M_{K^\pm})(\sqrt{M_{B_s}} - \sqrt{M_{K^\pm}})^2 \simeq 15.27$ GeV^2. Our pole factors will contain a single pole in both the vector and scalar channels, for which we take the mass values $M_{B^*} = 5.325$ GeV and $M_{B^*(0^+)} = 5.65$ GeV.[14]

We quote as our preferred result the outcome of the $N^+ = N^0 = 3$ BCL fit:

$B_s \to K$ ($N_f = 2 + 1$)

	Central Values	Correlation Matrix				
a_0^+	0.360(14)	1	0.098	-0.216	0.730	0.345
a_1^+	-0.828(83)	0.098	1	0.459	0.365	0.839
a_2^+	1.11(55)	-0.216	0.459	1	0.263	0.6526
a_0^0	0.233(10)	0.730	0.365	0.263	1	0.506
a_1^0	0.197(81)	0.345	0.839	0.652	0.506	1

where the uncertainties on a_0 and a_1 encompass the central values obtained from $\mathcal{O}(z^2)$ fits, and thus adequately reflect the systematic uncertainty on those series coefficients.[15] These can be used as the averaged FLAG results for the lattice-computed form factors $f_+(q^2)$ and $f_0(q^2)$. The coefficient a_3^+ can be obtained from the values for a_0^+–a_2^+ using Eq. (187). The fit is illustrated in Fig. 25.

8.3.4 Form factors for rare and radiative B-semileptonic decays to light flavours

Lattice-QCD input is also available for some exclusive semileptonic decay channels involving neutral-current $b \to q$ transitions at the quark level, where $q = d, s$. Being forbidden at tree level in the SM, these processes allow for stringent tests of potential new physics; simple examples are $B \to K^*\gamma$, $B \to K^{(*)}\ell^+\ell^-$, or $B \to \pi\ell^+\ell^-$ where the B meson (and therefore the light meson in the final state) can be either neutral or charged.

The corresponding SM effective weak Hamiltonian is considerably more complicated than the one for the tree-level processes discussed above: after neglecting top-quark effects, as many as ten dimension-six operators formed by the product of two hadronic currents or one hadronic and one leptonic current appear.[16] Three of the latter, coming from penguin and box diagrams, dominate at short distances and have matrix elements that, up to small QED corrections, are given entirely in terms of $B \to (\pi, K, K^*)$ form factors. The matrix elements of the remaining seven operators can be expressed, up to power corrections whose size is still unclear, in terms of form factors, decay constants and light-cone distribution amplitudes (for

[14] The values of the scalar resonance mass in $B\pi$ scattering taken by HPQCD and RBC/UKQCD are $M_{B^*(0^+)} = 5.6794(10)$ GeV and $M_{B^*(0^+)} = 5.63$ GeV, respectively. We use an average of the two values, and have checked that changing it by $\sim 1\%$ has a negligible impact on the fit results.

[15] In this case, $\mathcal{O}(z^4)$ fits with just two degrees of freedom, are significantly less stable. Still, the results for a_0^+ and a_1^+ are always compatible with the ones at $\mathcal{O}(z^2)$ and $\mathcal{O}(z^3)$ within one standard deviation.

[16] See, e.g., Ref. [92] and references therein.

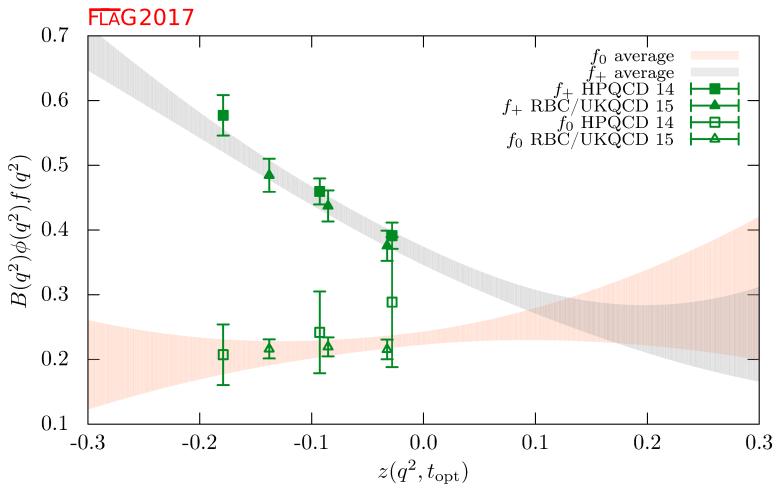

Figure 25: The form factors $(1 - q^2/m^2_{B^*})f_+(q^2)$ and $(1 - q^2/m^2_{B^*(0+)})f_0(q^2)$ for $B_s \to K\ell\nu$ plotted versus z. (See text for a discussion of the datasets.) The grey and orange bands display our preferred $N^+ = N^0 = 3$ BCL fit (five parameters) to the plotted data with errors.

the π, K, K^* and B mesons) by employing OPE arguments (at large di-lepton invariant mass) and results from Soft Collinear Effective Theory (at small di-lepton invariant mass). In conclusion, the most important contributions to all of these decays are expected to come from matrix elements of current operators (vector, tensor, and axial-vector) between one-hadron states, which in turn can be parameterized in terms of a number of form factors (see Ref. [93] for a complete description).

In channels with pseudoscalar mesons in the final state, the level of sophistication of lattice calculations is similar to the $B \to \pi$ case and there are results for the vector, scalar, and tensor form factors for $B \to K\ell^+\ell^-$ decays by HPQCD [94], and (very recent) results for both $B \to \pi\ell^+\ell^-$ [96] and $B \to K\ell^+\ell^-$ [95] from FNAL/MILC. Full details about these two calculations are provided in Tab. 40 and in the tables in App. B.6.4. Both computations employ MILC $N_f = 2 + 1$ asqtad ensembles. HPQCD [97] and FNAL/MILC [98] have also companion papers in which they calculate the Standard Model predictions for the differential branching fractions and other observables and compare to experiment. The HPQCD computation employs NRQCD b quarks and HISQ valence light quarks, and parameterizes the form factors over the full kinematic range using a model-independent z-expansion as in Sec. 8.3.1, including the covariance matrix of the fit coefficients. In the case of the (separate) FNAL/MILC computations, both of them use Fermilab b quarks and asqtad light quarks, and a BCL z-parameterization of the form factors.

The averaging of the HPQCD and FNAL/MILC results is similar to our treatment of the $B \to \pi$ and $B_s \to K$ form factors. In this case, even though the statistical uncertainties are partially correlated because of some overlap between the adopted sets of MILC ensembles, we choose to treat the two calculations as independent. The reason is that, in $B \to K$, statistical uncertainties are subdominant and cannot be easily extracted from the results presented by HPQCD and FNAL/MILC. Both collaborations provide only the outcome of a simultaneous z-fit to the vector, scalar and tensor form factors, that we use to generate appropriate synthetic data. We then impose the kinematic constraint $f_+(q^2 = 0) = f_0(q^2 = 0)$

Collaboration	Ref.	N_f	publication status	continuum extrapolation	chiral extrapolation	finite volume	renormalization	heavy-quark treatment	z-parameterization
HPQCD 13E	[94]	2+1	A	○	○	○	○	✓	BCL
FNAL/MILC 15D	[95]	2+1	A	★	○	★	○	✓	BCL

Table 40: Results for the $B \to K$ semileptonic form factors.

and fit to ($N^+ = N^0 = N^T = 3$) BCL parametrization. The functional forms of the form factors that we use are identical to those adopted in Ref. [98].[17] Our results are:

$B \to K$ ($N_f = 2 + 1$)

	Central Values	Correlation Matrix							
a_0^+	0.4696 (97)	1	0.467	0.058	0.755	0.553	0.609	0.253	0.102
a_1^+	-0.73 (11)	0.467	1	0.643	0.770	0.963	0.183	0.389	0.255
a_2^+	0.39 (50)	0.058	0.643	1	0.593	0.749	-0.145	0.023	0.176
a_0^0	0.3004 (73)	0.755	0.770	0.593	1	0.844	0.379	0.229	0.187
a_1^0	0.42 (11)	0.553	0.963	0.749	0.844	1	0.206	0.325	0.245
a_0^T	0.454 (15)	0.609	0.183	-0.145	0.379	0.206	1	0.707	0.602
a_1^T	-1.00 (23)	0.253	0.389	0.023	0.229	0.325	0.707	1	0.902
a_2^T	-0.89 (96)	0.102	0.255	0.176	0.187	0.245	0.602	0.902	1

The fit is illustrated in Fig. 26. Note that the average for the f_T form factor appears to prefer the FNAL/MILC synthetic data. This happens because we perform a correlated fit of the three form factors simultaneously (both FNAL/MILC and HPQCD present covariance matrices that include correlations between all form factors). We checked that the average for the f_T form factor, obtained neglecting correlations with f_0 and f_+, is a little lower and lies in between the two data sets.

Lattice computations of form factors in channels with a vector meson in the final state face extra challenges with respect to the case of a pseudoscalar meson: the state is unstable, and the extraction of the relevant matrix element from correlation functions is significantly more complicated; χPT cannot be used as a guide to extrapolate results at unphysically heavy pion masses to the chiral limit. While the field theory procedures to take resonance effects into account are available [100–108], they have not yet been implemented in the existing preliminary computations, which therefore suffer from uncontrolled systematic errors in calculations of weak decay form factors into unstable vector meson final states, such as the

[17] Note in particular that not much is known about the sub-threshold poles for the scalar form factor. FNAL/MILC includes one pole at the B_{s0}^* mass as taken from the calculation in Ref. [99].

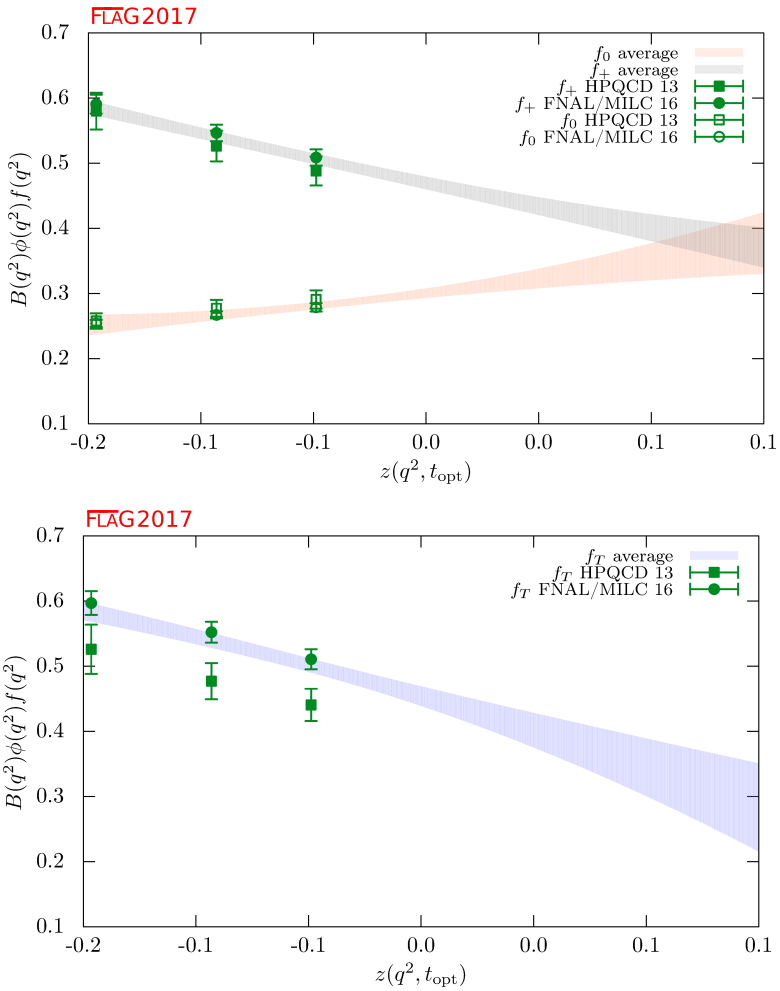

Figure 26: The $B \to K$ form factors $(1 - q^2/m^2_{B^*})f_+(q^2)$, $(1 - q^2/m^2_{B^*(0+)})f_0(q^2)$ and $(1 - q^2/m^2_{B^*})f_T(q^2)$ plotted versus z. (See text for a discussion of the datasets.) The grey, orange and blue bands display our preferred $N^+ = N^0 = N^T = 3$ BCL fit (eight parameters) to the plotted data with errors.

K^* or ρ mesons.[18]

As a consequence of the complexity of the problem, the level of maturity of these computations is significantly below the one present for pseudoscalar form factors. Therefore, we will only provide below a short guide to the existing results.

Concerning channels with vector mesons in the final state, Horgan *et al.* have obtained the seven form factors governing $B \to K^* \ell^+ \ell^-$ (as well as those for $B_s \to \phi \ell^+ \ell^-$) in Ref. [109] using NRQCD b quarks and asqtad staggered light quarks. In this work, they use a modified z-expansion to simultaneously extrapolate to the physical light-quark masses and continuum and extrapolate in q^2 to the full kinematic range. As discussed in Sec. 7.2, the modified z-expansion is not based on an underlying effective theory, and the associated uncertainties have yet to be fully studied. Horgan *et al.* use their form-factor results to calculate the differential branching fractions and angular distributions and discuss the implications for phenomenology in a companion paper [110]. Finally, ongoing work on $B \to K^* \ell^+ \ell^-$ and $B_s \to \phi \ell^+ \ell^-$ by RBC/UKQCD, including first results, have recently been reported in Ref. [111].

8.4 Semileptonic form factors for $B \to D\ell\nu$, $B \to D^*\ell\nu$, and $B \to D\tau\nu$

The semileptonic processes $B \to D\ell\nu$ and $B \to D^*\ell\nu$ have been studied extensively by experimentalists and theorists over the years. They allow for the determination of the CKM matrix element $|V_{cb}|$, an extremely important parameter of the Standard Model. $|V_{cb}|$ appears in many quantities that serve as inputs into CKM Unitarity Triangle analyses and reducing its uncertainties is of paramount importance. For example, when ϵ_K, the measure of indirect CP violation in the neutral kaon system, is written in terms of the parameters ρ and η that specify the apex of the unitarity triangle, a factor of $|V_{cb}|^4$ multiplies the dominant term. As a result, the errors coming from $|V_{cb}|$ (and not those from B_K) are now the dominant uncertainty in the Standard Model (SM) prediction for this quantity.

The decay rates for $B \to D^{(*)}\ell\nu$ can be parameterized in terms of vector and scalar form factors in the same way as, e.g., $B \to \pi\ell\nu$, see Sec. 8.3. Traditionally, the light channels $\ell = e,\ \mu$ have however been dealt with using a somewhat different notation, viz.

$$\frac{d\Gamma_{B^- \to D^0 \ell^- \bar{\nu}}}{dw} = \frac{G_F^2 m_D^3}{48\pi^3}(m_B + m_D)^2 (w^2-1)^{3/2} |\eta_{\rm EW}|^2 |V_{cb}|^2 |\mathcal{G}(w)|^2, \tag{191}$$

$$\frac{d\Gamma_{B^- \to D^{0*} \ell^- \bar{\nu}}}{dw} = \frac{G_F^2 m_{D^*}^3}{4\pi^3}(m_B - m_{D^*})^2 (w^2-1)^{1/2} |\eta_{\rm EW}|^2 |V_{cb}|^2 \chi(w) |\mathcal{F}(w)|^2, \tag{192}$$

where $w \equiv v_B \cdot v_{D^{(*)}}$, $v_P = p_P/m_P$ are the four-velocities of the mesons, and $\eta_{\rm EW} = 1.0066$ is the 1-loop electroweak correction [112]. The function $\chi(w)$ in Eq. (192) depends upon the recoil w and the meson masses, and reduces to unity at zero recoil [92]. These formulas do not include terms that are proportional to the lepton mass squared, which can be neglected for $\ell = e, \mu$. Until recently, most unquenched lattice calculations for $B \to D^*\ell\nu$ and $B \to D\ell\nu$ decays focused on the form factors at zero recoil $\mathcal{F}^{B\to D^*}(1)$ and $\mathcal{G}^{B\to D}(1)$; these can then be combined with experimental input to extract $|V_{cb}|$. The main reasons for concentrating on the zero recoil point are that (i) the decay rate then depends on a single form factor, and (ii) for $B \to D^*\ell\nu$, there are no $\mathcal{O}(\Lambda_{QCD}/m_Q)$ contributions due to Luke's theorem [113]. Further, the zero recoil form factor can be computed via a double ratio in which most of the current renormalization cancels and heavy-quark discretization errors are suppressed by an additional power of Λ_{QCD}/m_Q. Recent work on $B \to D^{(*)}\ell\nu$ transitions has started to

[18] In cases such as $B \to D^*$ transitions, that will be discussed below, this is much less of a practical problem due to the very narrow nature of the resonance.

explore the dependence of the relevant form factors on the momentum transfer, using a similar methodology to the one employed in $B \to \pi\ell\nu$ transitions; we refer the reader to Sec. 8.3 for a detailed discussion.

At the time of the previous version of this review, there were no published complete computations of the form factors for $B \to D\ell\nu$ decays: $N_f = 2+1$ results by FNAL/MILC for $\mathcal{G}^{B\to D}(1)$ had only appeared in proceedings form [114, 115], while the (now published) $N_f = 2$ study by Atoui *et al.* [116], that in addition to providing $\mathcal{G}^{B\to D}(1)$ explores the $w > 1$ region, was still in preprint form. This latter work also provided the first results for $B_s \to D_s\ell\nu$ amplitudes, again including information about the momentum transfer dependence; this will allow for an independent determination of $|V_{cb}|$ as soon as experimental data are available for these transitions. Meanwhile, the only fully published unquenched results for $\mathcal{F}^{B\to D^*}(1)$, obtained by FNAL/MILC, dated from 2008 [117]. In the last two years, however, significant progress has been attained in $N_f = 2+1$ computations: the FNAL/MILC value for $\mathcal{F}^{B\to D^*}(1)$ has been updated in Ref. [118], and full results for $B \to D\ell\nu$ at $w \geq 1$ have been published by FNAL/MILC [119] and HPQCD [120]. These works also provide full results for the scalar form factor, allowing us to analyze the decay in the τ channel. In the discussion below, we will only refer to this latest generation of results, which supersedes previous $N_f = 2+1$ determinations and allows for an extraction of $|V_{cb}|$ that incorporates information about the q^2 dependence of the decay rate (cf. Sec. 8.7).

8.4.1 $B_{(s)} \to D_{(s)}$ decays

We will first discuss the $N_f = 2+1$ computations of $B \to D\ell\nu$ by FNAL/MILC and HPQCD mentioned above, both based on MILC asqtad ensembles. Full details about all the computations are provided in Tab. 41 and in the tables in App. B.6.5.

The FNAL/MILC study [119] employs ensembles at four values of the lattice spacing ranging between approximately 0.045 fm and 0.12 fm, and several values of the light-quark mass corresponding to pions with RMS masses ranging between 260 MeV and 670 MeV (with just one ensemble with $M_\pi^{\rm RMS} \simeq 330$ MeV at the finest lattice spacing). The b and c quarks are treated using the Fermilab approach. The quantities directly studied are the form factors $h_\pm$ defined by

$$\frac{\langle D(p_D)|i\bar{c}\gamma_\mu b|B(p_B)\rangle}{\sqrt{m_D m_B}} = h_+(w)(v_B + v_D)_\mu + h_-(w)(v_B - v_D)_\mu \,, \tag{193}$$

which are related to the standard vector and scalar form factors by

$$f_+(q^2) = \tfrac{1}{2\sqrt{r}}\left[(1+r)h_+(w) - (1-r)h_-(w)\right] , \qquad f_0(q^2) = \sqrt{r}\left[\tfrac{1+w}{1+r}\,h_+(w) + \tfrac{1-w}{1-r}\,h_-(w)\right] , \tag{194}$$

with $r = m_D/m_B$. (Recall that $q^2 = (p_B - p_D)^2 = m_B^2 + m_D^2 - 2wm_Bm_D$.) The hadronic form factor relevant for experiment, $\mathcal{G}(w)$, is then obtained from the relation $\mathcal{G}(w) = 4rf_+(q^2)/(1+r)$. The form factors are obtained from double ratios of three-point functions in which the flavour-conserving current renormalization factors cancel. The remaining matching factor $\rho_{V^\mu_{cb}}$ is estimated with 1-loop lattice perturbation theory. In order to obtain $h_\pm(w)$, a joint continuum-chiral fit is performed to an ansatz that contains the light-quark mass and lattice spacing dependence predicted by next-to-leading order HMrSχPT, and the leading dependence on m_c predicted by the heavy-quark expansion ($1/m_c^2$ for h_+ and $1/m_c$ for h_-). The w-dependence, which allows for an interpolation in w, is given by analytic terms up to $(1-w)^2$,

as well as a contribution from the log proportional to $g^2_{D^*D\pi}$. The total resulting systematic error is 1.2% for f_+ and 1.1% for f_0. This dominates the final error budget for the form factors. After f_+ and f_0 have been determined as functions of w within the interval of values of q^2 covered by the computation, synthetic data points are generated to be subsequently fitted to a z-expansion of the BGL form, cf. Sec. 8.3, with pole factors set to unity. This in turn enables one to determine $|V_{cb}|$ from a joint fit of this z-expansion and experimental data. The value of the zero-recoil form factor resulting from the z-expansion is

$$\mathcal{G}^{B\to D}(1) = 1.054(4)_{\rm stat}(8)_{\rm sys}\,. \tag{195}$$

The HPQCD computation [120] considers ensembles at two values of the lattice spacing, $a = 0.09,\ 0.12$ fm, and two and three values of light-quark masses, respectively. The b quark is treated using NRQCD, while for the c quark the HISQ action is used. The form factors studied, extracted from suitable three-point functions, are

$$\langle D(p_D)|V^0|B\rangle = \sqrt{2M_B}f_\parallel\,, \qquad \langle D(p_D)|V^k|B\rangle = \sqrt{2M_B}p^k_D f_\perp\,, \tag{196}$$

where V_μ is the relevant vector current and the B rest frame is assumed. The standard vector and scalar form factors are retrieved as

$$f_+ = \tfrac{1}{\sqrt{2M_B}}f_\parallel + \tfrac{1}{\sqrt{2M_B}}(M_B - E_D)f_\perp\,, \qquad f_0 = \tfrac{\sqrt{2M_B}}{M_B^2-M_D^2}\left[(M_B-E_D)f_\parallel + (M_B^2-E_D^2)f_\perp\right]\,. \tag{197}$$

The currents in the effective theory are matched at 1-loop to their continuum counterparts. Results for the form factors are then fitted to a modified BCL z-expansion ansatz, that takes into account simultaneously the lattice spacing, light-quark masses, and q^2 dependence. For the mass dependence NLO chiral logs are included, in the form obtained in hard-pion χPT. As in the case of the FNAL/MILC computation, once f_+ and f_0 have been determined as functions of q^2, $|V_{cb}|$ can be determined from a joint fit of this z-expansion and experimental data. The work quotes for the zero-recoil vector form factor the result

$$\mathcal{G}^{B\to D}(1) = 1.035(40)\,. \tag{198}$$

This value is 1.8σ smaller than the FNAL/MILC result and significantly less precise. The dominant source of errors in the $|V_{cb}|$ determination by HPQCD are discretization effects and the systematic uncertainty associated with the perturbative matching.

In order to combine the form factors determinations of HPQCD and FNAL/MILC into a lattice average, we proceed in a similar way as with $B\to\pi\ell\nu$ and $B_s\to K\ell\nu$ above. FNAL/MILC quotes synthetic values for the form factors at three values of w (or, alternatively, q^2) with a full correlation matrix, which we take directly as input. In the case of HPQCD, we use their preferred modified z-expansion parameterization to produce synthetic values of the form factors at two different values of q^2. This leaves us with a total of five data points in the kinematical range $w\in[1.00, 1.11]$. As in the case of $B\to\pi\ell\nu$, we conservatively assume a 100% correlation of statistical uncertainties between HPQCD and FNAL/MILC. We then fit this dataset to a BCL ansatz, using $t_+ = (M_{B^0}+M_{D^\pm})^2 \simeq 51.12$ GeV^2 and $t_0 = (M_{B^0}+M_{D^\pm})(\sqrt{M_{B^0}}-\sqrt{M_{D^\pm}})^2 \simeq 6.19$ GeV^2. In our fits, pole factors have been set to unity — i.e., we do not take into account the effect of sub-threshold poles, which is then implicitly absorbed into the series coefficients. The reason for this is our imperfect knowledge

of the relevant resonance spectrum in this channel, which does not allow us to decide the precise number of poles needed.[19] This in turn implies that unitarity bounds do not rigorously apply, which has to be taken into account when interpreting the results (cf. Sec. 8.3.1).

With a procedure similar to what we adopted for the $B \to \pi$ and $B_s \to K$ cases, we impose the kinematic constraint at $q^2 = 0$ by expressing the $a^0_{N^0-1}$ coefficient in the z-expansion of f_0 in terms of all other coefficients. As mentioned above FNAL/MILC provides synthetic data for f_+ and f_0 including correlations; HPQCD presents the result of simultaneous z-fits to the two form factors including all correlations and, thus enabling us to generate a complete set of synthetic data for f_+ and f_0. Since both calculations are based on MILC ensembles, we then reconstruct the off-diagonal HPQCD-FNAL/MILC entries of the covariance matrix by conservatively assuming that statistical uncertainties are 100% correlated. The Fermilab/MILC (HPQCD) statistical error is 58% (31%) for every f_+ value and 64% (49%) for every f_0 one. Using this information we can easily build the off-diagonal block of the overall covariance matrix (e.g., the covariance between $[f_+(q^2_1)]_{\rm FNAL}$ and $[f_0(q^2_2)]_{\rm HPQCD}$ is $(\delta[f_+(q^2_1)]_{\rm FNAL} \times 0.58)$ $(\delta[f_0(q^2_2)]_{\rm HPQCD} \times 0.49)$, where δf is the total error).

For our central value, we choose an $N^+ = N^0 = 3$ BCL fit:

$B \to D$ ($N_f = 2 + 1$)

a^i_n	Central Values	Correlation Matrix				
a^+_0	0.909 (14)	1	0.737	0.594	0.976	0.777
a^+_1	-7.11 (65)	0.737	1	0.940	0.797	0.992
a^+_2	66 (11)	0.594	0.940	1	0.666	0.938
a^0_0	0.794 (12)	0.976	0.797	0.666	1	0.818
a^0_1	-2.45 (65)	0.777	0.992	0.938	0.818	1

where the coefficient a^+_3 can be obtained from the values for a^+_0–a^+_2 using Eq. (187). The fit is illustrated in Fig. 27.

Ref. [116] is the only existing $N_f = 2$ work on $B \to D\ell\nu$ transitions, that furthermore provides the only available results for $B_s \to D_s\ell\nu$. This computation uses the publicly available ETM configurations obtained with the twisted-mass QCD action at maximal twist. Four values of the lattice spacing, ranging between 0.054 fm and 0.098 fm, are considered, with physical box lengths ranging between 1.7 fm and 2.7 fm. At two values of the lattice spacing two different physical volumes are available. Charged-pion masses range between ≈ 270 MeV and ≈ 490 MeV, with two or three masses available per lattice spacing and volume, save for the $a \approx 0.054$ fm point at which only one light mass is available for each of the two volumes. The strange and heavy valence quarks are also treated with maximally twisted-mass QCD.

The quantities of interest are again the form factors $h_\pm$ defined above. In order to control discretization effects from the heavy quarks, a strategy similar to the one employed by the ETM Collaboration in their studies of B-meson decay constants (cf. Sec. 8.1) is employed: the value of $\mathcal{G}(w)$ is computed at a fixed value of m_c and several values of a heavier quark mass $m^{(k)}_h = \lambda^k m_c$, where λ is a fixed scaling parameter, and step-scaling functions are built as

$$\Sigma_k(w) = \frac{\mathcal{G}(w, \lambda^{k+1} m_c, m_c, a^2)}{\mathcal{G}(w, \lambda^k m_c, m_c, a^2)} \,. \tag{199}$$

[19] As noted above, this is the same approach adopted by FNAL/MILC in their fits to a BGL ansatz. HPQCD, meanwhile, uses one single pole in the pole factors that enter their modified z-expansion, using their spectral studies to fix the value of the relevant resonance masses.

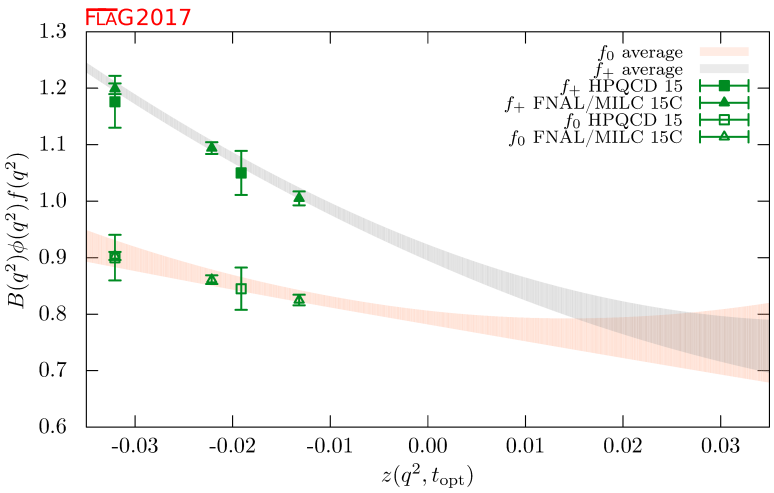

Figure 27: The form factors $f_+(q^2)$ and $f_0(q^2)$ for $B \to D\ell\nu$ plotted versus z. (See text for a discussion of the datasets.) The grey and orange bands display our preferred $N^+ = N^0 = 3$ BCL fit (five parameters) to the plotted data with errors.

Each ratio is extrapolated to the continuum limit, $\sigma_k(w) = \lim_{a\to 0} \Sigma_k(w)$. One then exploits the fact that the $m_h \to \infty$ limit of the step-scaling is fixed — in particular, it is easy to find from the heavy-quark expansion that $\lim_{m_h\to\infty} \sigma(1) = 1$. In this way, the physical result at the b-quark mass can be reached by interpolating $\sigma(w)$ between the charm region (where the computation can be carried out with controlled systematics) and the known static limit value.

In practice, the values of m_c and m_s are fixed at each value of the lattice spacing such that the experimental kaon and D_s masses are reached at the physical point, as determined in Ref. [121]. For the scaling parameter, $\lambda = 1.176$ is chosen, and eight scaling steps are performed, reaching $m_h/m_c = 1.176^9 \simeq 4.30$, approximately corresponding to the ratio of the physical b- and c-masses in the $\overline{\rm MS}$ scheme at 2 GeV. All observables are obtained from ratios that do not require (re)normalization. The ansatz for the continuum and chiral extrapolation of Σ_k contains a constant and linear terms in $m_{\rm sea}$ and a^2. Twisted boundary conditions in space are used for valence-quark fields for better momentum resolution. Applying this strategy the form factors are finally obtained at four reference values of w between 1.004 and 1.062, and, after a slight extrapolation to $w = 1$, the result is quoted

$$\mathcal{G}^{B_s\to D_s}(1) = 1.052(46)\,. \tag{200}$$

The authors also provide values for the form factor relevant for the meson states with light valence quarks, obtained from a similar analysis to the one described above for the $B_s \to D_s$ case. Values are quoted from fits with and without a linear $m_{\rm sea}/m_s$ term in the chiral extrapolation. The result in the former case, which safely covers systematic uncertainties, is

$$\mathcal{G}^{B\to D}(1) = 1.033(95)\,. \tag{201}$$

Given the identical strategy, and the small sensitivity of the ratios used in their method to the light valence- and sea-quark masses, we assign this result the same ratings in Tab. 41 as those for their calculation of $\mathcal{G}^{B_s\to D_s}(1)$. Currently the precision of this calculation is not competitive with that of $N_f = 2+1$ works, but this is due largely to the small number

of configurations analysed by Atoui *et al.* The viability of their method has been clearly demonstrated, however, which leaves significant room for improvement on the errors of both the $B \to D$ and $B_s \to D_s$ form factors with this approach by including either additional two-flavour data or analysing more recent ensembles with $N_f > 2$.

Finally, Atoui *et al.* also study the scalar and tensor form factors, as well as the momentum transfer dependence of $f_{+,0}$. The value of the ratio $f_0(q^2)/f_+(q^2)$ is provided at a reference value of q^2 as a proxy for the slope of $\mathcal{G}(w)$ around the zero-recoil limit.

8.4.2 Ratios of $B \to D\ell\nu$ form factors

The availability of results for the scalar form factor f_0 in the latest generation of results for $B \to D\ell\nu$ amplitudes allows us to study interesting observables that involve the decay in the τ channel. One such quantity is the ratio

$$R(D) = \mathcal{B}(B \to D\tau\nu)/\mathcal{B}(B \to D\ell\nu) \qquad \text{with } \ell = e, \mu\,, \tag{202}$$

which is sensitive to f_0, and can be accurately determined by experiment.[20] Indeed, the recent availability of experimental results for $R(D)$ has made this quantity particularly relevant in the search for possible physics beyond the Standard Model. Both FNAL/MILC and HPQCD provide values for $R(D)$ from their recent form factor computations, discussed above. In the FNAL/MILC case, this result supersedes their 2012 determination, which was discussed in the previous version of this review. The quoted values by FNAL/MILC and HPQCD are

$$R(D) = 0.299(11) \text{ Ref. [119]}\,, \qquad R(D) = 0.300(8) \text{ Ref. [120]}\,. \tag{203}$$

These results are in excellent agreement, and can be averaged (using the same considerations for the correlation between the two computations as we did in the averaging of form factors) into

$$R(D) = 0.300(8)\,, \qquad \text{our average.} \tag{204}$$

This result is about 1.6σ lower than the current experimental average for this quantity. It has to be stressed that achieving this level of precision critically depends on the reliability with which the low-q^2 region is controlled by the parameterizations of the form factors.

Another area of immediate interest in searches for physics beyond the Standard Model is the measurement of $B_s \to \mu^+\mu^-$ decays, recently achieved by LHCb.[21] In addition to the B_s decay constant (see Sec. 8.1), one of the hadronic inputs required by the LHCb analysis is the ratios of B_q meson ($q = d, s$) fragmentation fractions, f_s/f_d. A dedicated $N_f = 2 + 1$ study by FNAL/MILC[22] Ref. [122] addresses the ratios of scalar form factors $f_0^{(q)}(q^2)$, and quotes:

$$f_0^{(s)}(M_\pi^2)/f_0^{(d)}(M_K^2) = 1.046(44)(15), \qquad f_0^{(s)}(M_\pi^2)/f_0^{(d)}(M_\pi^2) = 1.054(47)(17), \tag{205}$$

where the first error is statistical and the second systematic. These results lead to fragmentation fraction ratios f_s/f_d that are consistent with LHCb's measurements via other methods [123].

[20] A similar ratio $R(D^*)$ can be considered for $B \to D^*$ transitions — as a matter of fact, the experimental value of $R(D^*)$ is significantly more accurate than the one of $R(D)$. However, the absence of lattice results for the $B \to D^*$ scalar form factor, and indeed of results at nonzero recoil (see below), takes $R(D^*)$ out of our current scope.

[21] See Ref. [1] for the latest results, obtained from a joint analysis of CMS and LHCb data.

[22] This work also provided a value for $R(D)$, now superseded by Ref. [119].

8.4.3 $B \to D^*$ decays

The most precise computation of the zero-recoil form factors needed for the determination of $|V_{cb}|$ from exclusive B semileptonic decays comes from the $B \to D^* \ell\nu$ form factor at zero recoil, $\mathcal{F}^{B\to D^*}(1)$, calculated by the FNAL/MILC Collaboration. The original computation, published in Ref. [117], has now been updated [118] by employing a much more extensive set of gauge ensembles and increasing the statistics of the ensembles originally considered, while preserving the analysis strategy. There is currently no unquenched computation of the relevant form factors at nonzero recoil.

This work uses the MILC $N_f = 2 + 1$ ensembles. The bottom and charm quarks are simulated using the clover action with the Fermilab interpretation and light quarks are treated via the asqtad staggered fermion action. At zero recoil $\mathcal{F}^{B\to D^*}(1)$ reduces to a single form factor $h_{A_1}(1)$ coming from the axial-vector current

$$\langle D^*(v,\epsilon')|\mathcal{A}_\mu|\overline{B}(v)\rangle = i\sqrt{2m_B 2m_{D^*}}\ \epsilon'^*_\mu h_{A_1}(1), \tag{206}$$

where ϵ' is the polarization of the D^*. The form factor is accessed through a ratio of three-point correlators, viz.

$$\mathcal{R}_{A_1} = \frac{\langle D^*|\bar{c}\gamma_j\gamma_5 b|\overline{B}\rangle\ \langle\overline{B}|\bar{b}\gamma_j\gamma_5 c|D^*\rangle}{\langle D^*|\bar{c}\gamma_4 c|D^*\rangle\ \langle\overline{B}|\bar{b}\gamma_4 b|\overline{B}\rangle} = |h_{A_1}(1)|^2. \tag{207}$$

Simulation data are obtained on MILC ensembles with five lattice spacings, ranging from $a \approx 0.15$ fm to $a \approx 0.045$ fm, and as many as five values of the light-quark masses per ensemble (though just one at the finest lattice spacing). Results are then extrapolated to the physical, continuum/chiral, limit employing staggered χPT.

The D^* meson is not a stable particle in QCD and decays predominantly into a D plus a pion. Nevertheless, heavy-light meson χPT can be applied to extrapolate lattice simulation results for the $B \to D^*\ell\nu$ form factor to the physical light-quark mass. The D^* width is quite narrow, 0.096 MeV for the $D^{*\pm}(2010)$ and less than 2.1MeV for the $D^{*0}(2007)$, making this system much more stable and long lived than the ρ or the K^* systems. The fact that the $D^* - D$ mass difference is close to the pion mass leads to the well known "cusp" in $\mathcal{R}_{A_1}$ just above the physical pion mass [124–126]. This cusp makes the chiral extrapolation sensitive to values used in the χPT formulas for the $D^*D\pi$ coupling $g_{D^*D\pi}$. The error budget in Ref. [118] includes a separate error of 0.3% coming from the uncertainty in $g_{D^*D\pi}$ in addition to general chiral extrapolation errors in order to take this sensitivity into account.

The final updated value presented in Ref. [118], that we quote as our average for this quantity, is

$$\mathcal{F}^{B\to D^*}(1) = h_{A_1}(1) = 0.906(4)(12)\,, \tag{208}$$

where the first error is statistical, and the second the sum of systematic errors added in quadrature, making up a total error of 1.4% (down from the original 2.6% of Ref. [117]). The largest systematic uncertainty comes from discretization errors followed by effects of higher-order corrections in the chiral perturbation theory ansatz.

8.5 Semileptonic form factors for $\Lambda_b \to p\ell\nu$ and $\Lambda_b \to \Lambda_c\ell\nu$

A recent new development in Lattice QCD computations for heavy-quark physics is the study of semileptonic decays of the Λ_b baryon, with first unquenched results provided in a work by Detmold, Lehner and Meinel [127]. The importance of this result is that, together with

Collaboration	Ref.	N_f	publication status	continuum extrapolation	chiral extrapolation	finite volume	renormalization	heavy-quark treatment	$w = 1$ form factor / ratio	
FNAL/MILC 14	[118]	2+1	A	★	○	★	○	✓	$\mathcal{F}^{B\to D^*}(1)$	0.906(4)(12)
HPQCD 15	[120]	2+1	A	○	○	○	○	✓	$\mathcal{G}^{B\to D}(1)$	1.035(40)
FNAL/MILC 15C	[119]	2+1	A	★	○	★	○	✓	$\mathcal{G}^{B\to D}(1)$	1.054(4)(8)
HPQCD 15	[120]	2+1	A	○	○	○	○	✓	$R(D)$	0.300(8)
FNAL/MILC 15C	[119]	2+1	A	★	○	★	○	✓	$R(D)$	0.299(11)
Atoui 13	[116]	2	A	★	○	★	—	✓	$\mathcal{G}^{B\to D}(1)$	1.033(95)
Atoui 13	[116]	2	A	★	○	★	—	✓	$\mathcal{G}^{B_s\to D_s}(1)$	1.052(46)

Table 41: Lattice results for the $B \to D^*\ell\nu$, $B \to D\ell\nu$, and $B_s \to D_s\ell\nu$ semileptonic form factors and $R(D)$.

a recent analysis by LHCb of the ratio of decay rates $\Gamma(\Lambda_b \to p\ell\nu)/\Gamma(\Lambda_b \to \Lambda_c\ell\nu)$ [128], it allows for an exclusive determination of the ratio $|V_{ub}|/|V_{cb}|$ largely independent from the outcome of different exclusive channels, thus contributing a very interesting piece of information to the existing tensions in the determination of third-column CKM matrix elements (cf. Secs. 8.6,8.7). For that reason, we will discuss these results briefly, notwithstanding the fact that baryon physics is in general out of the scope of the present review.

The amplitudes of the decays $\Lambda_b \to p\ell\nu$ and $\Lambda_b \to \Lambda_c\ell\nu$ receive contributions from both the vector and the axial components of the current in the matrix elements $\langle p|\bar{q}\gamma^\mu(\mathbf{1}-\gamma_5)b|\Lambda_b\rangle$ and $\langle\Lambda_c|\bar{q}\gamma^\mu(\mathbf{1}-\gamma_5)b|\Lambda_b\rangle$, and can be parameterized in terms of six different form factors — see, e.g., Ref. [129] for a complete description. They split into three form factors f_+, f_0, $f_\perp$ in the parity-even sector, mediated by the vector component of the current, and another three form factors $g_+, g_0, g_\perp$ in the parity-odd sector, mediated by the axial component. All of them provide contributions that are parametrically comparable.

The computation of Detmold *et al.* uses RBC/UKQCD $N_f = 2+1$ DWF ensembles, and treats the b and c quarks within the Columbia RHQ approach. Two values of the lattice spacing ($a \sim 0.112,\ 0.085$ fm) are considered, with the absolute scale set from the $\Upsilon(2S)$–$\Upsilon(1S)$ splitting. Sea pion masses lie in a narrow interval ranging from slightly above 400 MeV to slightly below 300 MeV, keeping $m_\pi L \gtrsim 4$; however, lighter pion masses are considered in the valence DWF action for the u, d quarks, leading to partial quenching effects in the chiral extrapolation. More importantly, this also leads to values of $M_{\pi,\mathrm{min}}L$ close to 3.0 (cf. App B.6.3 for details); compounded with the fact that there is only one lattice volume in

the computation, an application of the FLAG criteria would lead to a ■ rating for finite volume effects. It has to be stressed, however, that our criteria have been developed in the context of meson physics, and their application to the baryon sector is not straightforward; as a consequence, we will refrain from providing a conclusive rating of this computation for the time being.

Results for the form factors are obtained from suitable three-point functions, and fitted to a modified z-expansion ansatz that combines the q^2 dependence with the chiral and continuum extrapolations. The main results of the paper are the predictions (errors are statistical and systematic, respectively)

$$\begin{aligned} \frac{1}{|V_{ub}|^2}\int_{15\ \mathrm{GeV}^2}^{q^2_{\mathrm{max}}} \frac{\mathrm{d}\Gamma(\Lambda_b\to p\mu^-\bar\nu_\mu)}{\mathrm{d}q^2}\,\mathrm{d}q^2 &= 12.32(93)(80)\ \mathrm{ps}^{-1}\,, \\ \frac{1}{|V_{cb}|^2}\int_{15\ \mathrm{GeV}^2}^{q^2_{\mathrm{max}}} \frac{\mathrm{d}\Gamma(\Lambda_b\to \Lambda_c\mu^-\bar\nu_\mu)}{\mathrm{d}q^2}\,\mathrm{d}q^2 &= 8.39(18)(32)\ \mathrm{ps}^{-1}\,, \end{aligned} \tag{209}$$

which are the input for the LHCb analysis. Prediction for the total rates in all possible lepton channels, as well as for ratios similar to $R(D)$ (cf. Sec. 8.4) between the τ and light lepton channels are also available.

8.6 Determination of $|V_{ub}|$

We now use the lattice-determined Standard Model transition amplitudes for leptonic (Sec. 8.1) and semileptonic (Sec. 8.3) B-meson decays to obtain exclusive determinations of the CKM matrix element $|V_{ub}|$. In this section, we describe the aspect of our work that involves experimental input for the relevant charged-current exclusive decay processes. The relevant formulae are Eqs. (150) and (175). Among leptonic channels the only input comes from $B\to\tau\nu_\tau$, since the rates for decays to e and μ have not yet been measured. In the semileptonic case we only consider $B\to\pi\ell\nu$ transitions (experimentally measured for $\ell=e,\mu$). As discussed in Secs. 8.3 and 8.5, there are now lattice predictions for the rates of the decays $B_s\to K\ell\nu$ and $\Lambda_b\to p\ell\nu$; however, in the former case the process has not been experimentally measured yet, while in the latter case the only existing lattice computation does not meet FLAG requirements for controlled systematics.

We first investigate the determination of $|V_{ub}|$ through the $B\to\tau\nu_\tau$ transition. This is the only experimentally measured leptonic decay channel of the charged B-meson. After the publication of the previous FLAG report [11] in 2013, the experimental measurements of the branching fraction of this channel, $B(B^-\to\tau^-\bar\nu)$, were updated. While the results from the BaBar collaboration remain the same as those reported before the end of 2013, the Belle collaboration reanalysed the data and reported that the value of $B(B^-\to\tau^-\bar\nu)$ obtained with semileptonic tags changed from $1.54^{+0.38}_{-0.37}{}^{+0.29}_{-0.31}\times10^{-4}$ to $1.25\pm0.28\pm0.27\times10^{-4}$ [4]. Table 42 summarizes the current status of experimental results for this branching fraction.

It is obvious that all the measurements listed in Tab. 42 have significance less than 5σ, and the uncertainties are dominated by statistical errors. These measurements lead to the averages of experimental measurements for $B(B^-\to\tau\bar\nu)$ [3, 4],

$$\begin{aligned} B(B^-\to\tau\bar\nu) &= 0.91\pm0.22 \text{ from Belle,} \\ &= 1.79\pm0.48 \text{ from BaBar.} \end{aligned} \tag{210}$$

We notice that minor tension between results from the two collaborations can be observed, even in the presence of large errors. Despite this situation, in Ref. [2] the Particle Data Group

Collaboration	Tagging method	$B(B^- \to \tau^- \bar{\nu}) \times 10^4$
Belle [130]	Hadronic	$0.72^{+0.27}_{-0.25} \pm 0.11$
Belle [4]	Semileptonic	$1.25 \pm 0.28 \pm 0.27$
BaBar [3]	Hadronic	$1.83^{+0.53}_{-0.49} \pm 0.24$
BaBar [131]	Semileptonic	$1.7 \pm 0.8 \pm 0.2$

Table 42: Experimental measurements for $B(B^- \to \tau^- \bar{\nu})$. The first error on each result is statistical, while the second error is systematic.

performed a global average of $B(B^- \to \tau\bar{\nu})$ employing all the information in Tab. 42. Here we choose to proceed with the strategy of quoting different values of $|V_{ub}|$ as determined using inputs from the Belle and the BaBar experiments shown in Eq. (210), respectively.

Combining the results in Eq. (210) with the experimental measurements of the mass of the τ-lepton and the B-meson lifetime and mass, the Particle Data Group presented [2]

$$\begin{aligned} |V_{ub}| f_B &= 0.72 \pm 0.09 \text{ MeV from Belle,} \\ &= 1.01 \pm 0.14 \text{ MeV from BaBar,} \end{aligned} \tag{211}$$

which can be used to extract $|V_{ub}|$.

$$\begin{aligned} &N_f = 2 && \text{Belle } B \to \tau\nu_\tau : && |V_{ub}| = 3.83(48)(15) \times 10^{-3}\,, \\ &N_f = 2+1 && \text{Belle } B \to \tau\nu_\tau : && |V_{ub}| = 3.75(47)(9) \times 10^{-3}\,, \\ &N_f = 2+1+1 && \text{Belle } B \to \tau\nu_\tau : && |V_{ub}| = 3.87(48)(9) \times 10^{-3}\,; \\ &N_f = 2 && \text{Babar } B \to \tau\nu_\tau : && |V_{ub}| = 5.37(74)(21) \times 10^{-3}\,, \\ &N_f = 2+1 && \text{Babar } B \to \tau\nu_\tau : && |V_{ub}| = 5.26(73)(12) \times 10^{-3}\,, \\ &N_f = 2+1+1 && \text{Babar } B \to \tau\nu_\tau : && |V_{ub}| = 5.43(75)(12) \times 10^{-3}\,. \end{aligned} \tag{212}$$

where the first error comes from experiment and the second comes from the uncertainty in f_B.

Let us now turn our attention to semileptonic decays. The experimental value of $|V_{ub}| f_+(q^2)$ can be extracted from the measured branching fractions for $B^0 \to \pi^\pm \ell\nu$ and/or $B^\pm \to \pi^0 \ell\nu$ applying Eq. (175);[23] $|V_{ub}|$ can then be determined by performing fits to the constrained BCL z parameterization of the form factor $f_+(q^2)$ given in Eq. (188). This can be done in two ways: one option is to perform separate fits to lattice and experimental results, and extract the value of $|V_{ub}|$ from the ratio of the respective a_0 coefficients; a second option is to perform a simultaneous fit to lattice and experimental data, leaving their relative normalization $|V_{ub}|$ as a free parameter. We adopt the second strategy, because it combines the lattice and experimental input in a more efficient way, leading to a smaller uncertainty on $|V_{ub}|$.

The available state-of-the-art experimental input, as employed, e.g., by HFAG, consists of five datasets: three untagged measurements by BaBar (6-bin [132] and 12-bin [133]) and

[23] Since $\ell = e, \mu$ the contribution from the scalar form factor in Eq. (175) is negligible.

Belle [134], all of which assume isospin symmetry and provide combined $B^0 \to \pi^-$ and $B^+ \to \pi^0$ data; and the two tagged Belle measurements of $\bar{B}^0 \to \pi^+$ (13-bin) and $B^- \to \pi^0$ (7-bin) [135]. In the previous version of the FLAG review [11] we only used the 13-bin Belle and 12-bin BaBar datasets, and performed separate fits to them due to the lack of information on systematic correlations between them. Now however we will follow established practice, and perform a combined fit to all the experimental data. This is based on the existence of new information about cross-correlations, that allows us to obtain a meaningful final error estimate.[24] The lattice input dataset will be the same discussed in Sec. 8.3.

We perform a constrained BCL fit of the vector and scalar form factors (this is necessary in order to take into account the $f_+(q^2 = 0) = f_0(q^2)$ constraint) together with the combined experimental datasets. We find that the error on V_{ub} stabilizes for $(N^+ = N^0 = 3)$. The result of the combined fit is:

$B \to \pi\ell\nu$ $(N_f = 2 + 1)$

	Central Values	Correlation Matrix					
$V_{ub} \times 10^3$	3.73 (14)	1	0.852	0.345	-0.374	0.211	0.247
a_0^+	0.414 (12)	0.852	1	0.154	-0.456	0.259	0.144
a_1^+	-0.494 (44)	0.345	0.154	1	-0.797	-0.0995	0.223
a_2^+	-0.31 (16)	-0.374	-0.456	-0.797	1	0.0160	-0.0994
a_0^0	0.499 (19)	0.211	0.259	-0.0995	0.0160	1	-0.467
a_1^0	-1.426 (46)	0.247	0.144	0.223	-0.0994	-0.467	1

Fig. 28 shows both the lattice and experimental data for $(1-q^2/m^2_{B^*})f_+(q^2)$ as a function of $z(q^2)$, together with our preferred fit; experimental data have been rescaled by the resulting value for $|V_{ub}|^2$. It is worth noting the good consistency between the form factor shapes from lattice and experimental data. This can be quantified, e.g., by computing the ratio of the two leading coefficients in the constrained BCL parameterization: the fit to lattice form factors yields $a_1^+/a_0^+ = -1.67(12)$ (cf. the results presented in Sec. 8.3.2), while the above lattice+experiment fit yields $a_1^+/a_0^+ = -1.193(16)$.

We plot the values of $|V_{ub}|$ we have obtained in Fig. 30, where the determination through inclusive decays by the Heavy Flavour Averaging Group (HFAG) [7], yielding $|V_{ub}| = 4.62\ (20)(29) \times 10^{-3}$, is also shown for comparison. In this plot the tension between the BaBar and the Belle measurements of $B(B^- \to \tau^-\bar{\nu})$ is manifest. As discussed above, it is for this reason that we do not extract $|V_{ub}|$ through the average of results for this branching fraction from these two collaborations. In fact this means that a reliable determination of $|V_{ub}|$ using information from leptonic B-meson decays is still absent; the situation will only clearly improve with the more precise experimental data expected from Belle II. The value for $|V_{ub}|$ obtained from semileptonic B decays for $N_f = 2 + 1$, on the other hand, is significantly more precise than both the leptonic and the inclusive determinations, and exhibits the well-known $\sim 3\sigma$ tension with the latter.

8.7 Determination of $|V_{cb}|$

We will now use the lattice QCD results for the $B \to D^{(*)}\ell\nu$ form factors in order to obtain determinations of the CKM matrix element $|V_{cb}|$ in the Standard Model. The relevant formulae are given in Eq. (192).

[24] See, e.g., Sec. V.D of [83] for a detailed discussion.

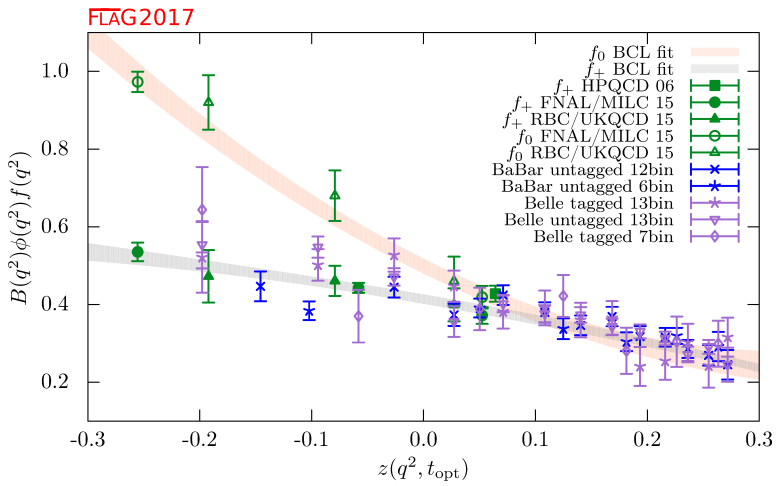

Figure 28: Lattice and experimental data for $(1 - q^2/m_{B^*}^2) f_+^{B\to\pi}(q^2)$ and $f_0^{B\to\pi}(q^2)$ versus z. Green symbols denote lattice-QCD points included in the fit, while blue and indigo points show experimental data divided by the value of $|V_{ub}|$ obtained from the fit. The grey and orange bands display the preferred $N^+ = N^0 = 3$ BCL fit (six parameters) to the lattice-QCD and experimental data with errors.

Let us summarize the lattice input that satisfies FLAG requirements for the control of systematic uncertainties, discussed in Sec. 8.4. In the (experimentally more precise) $B \to D^*\ell\nu$ channel, there is only one $N_f = 2+1$ lattice computation of the relevant form factor $\mathcal{F}^{B\to D^*}$ at zero recoil. Concerning the $B \to D\ell\nu$ channel, for $N_f = 2$ there is one determination of the relevant form factor $\mathcal{G}^{B\to D}$ at zero recoil[25]; while for $N_f = 2+1$ there are two determinations of the $B \to D$ form factor as a function of the recoil parameter in roughly the lowest third of the kinematically allowed region. In this latter case, it is possible to replicate the analysis carried out for $|V_{ub}|$ in Sec. 8.6, and perform a joint fit to lattice and experimental data; in the former, the value of $|V_{cb}|$ has to be extracted by matching to the experimental value for $\mathcal{F}^{B\to D^*}(1)\eta_{\rm EW}|V_{cb}|$ and $\mathcal{G}^{B\to D}(1)\eta_{\rm EW}|V_{cb}|$.

The latest experimental average by HFAG [7] for the $B \to D^*$ form factor at zero recoil is

$$\mathcal{F}^{B\to D^*}(1)\eta_{\rm EW}|V_{cb}| = 35.81(0.45) \times 10^{-3}\,. \tag{213}$$

By using $\eta_{\rm EW} = 1.00662$ [26] and the lattice value for $\mathcal{F}^{B\to D^*}(1)$ in Eq. (208), we thus extract our average

$$N_f = 2+1 \qquad B \to D^*\ell\nu: \qquad |V_{cb}| = 39.27(56)(49) \times 10^{-3}\,, \tag{214}$$

where the first uncertainty comes from the lattice computation and the second from the experimental input. For the zero-recoil $B \to D$ form factor, HFAG quotes

$$\text{HFAG:} \qquad \mathcal{G}^{B\to D}(1)\eta_{\rm EW}|V_{cb}| = 42.65(1.53) \times 10^{-3}\,. \tag{215}$$

[25] The same work provides $\mathcal{G}^{B_s\to D_s}$, for which there are, however, no experimental data.

[26] Note that this determination does not include the electromagnetic Coulomb correction roughly estimated in Ref. [118]. Currently the numerical impact of this correction is negligible.

This average is strongly dominated by the BaBar input. The set of experimental results for $B \to D\ell\nu$ has however been significantly improved by the recent publication of a new Belle measurement [564], which quotes

$$\text{Belle 2016:} \qquad \mathcal{G}^{B\to D}(1)\eta_{\rm EW}|V_{cb}| = 42.29(1.37)\times 10^{-3}\,. \tag{216}$$

Given the difficulties to include this latter number in a global average replicating the procedure followed by HFAG, and the fact that the final uncertainty will be completely dominated by the error of the lattice input in Eq. (201), we will conservatively use the value in Eq. (215) to provide an average for $N_f = 2$, and quote

$$N_f = 2 \qquad\qquad B \to D\ell\nu: \qquad\qquad |V_{cb}| = 41.0(3.8)(1.5)\times 10^{-3}\,. \tag{217}$$

Finally, for $N_f = 2+1$ we will perform, as discussed above, a joint fit to the available lattice data, discussed in Sec. 8.4, and state-of-the-art experimental determinations. In this case we will combine the aforementioned recent Belle measurement [564], which provides partial integrated decay rates in 10 bins in the recoil parameter w, with the 2010 BaBar dataset in Ref. [137], which quotes the value of $\mathcal{G}^{B\to D}(w)\eta_{\rm EW}|V_{cb}|$ for ten values of w.[27] The fit is dominated by the more precise Belle data; given this, and the fact that only partial correlations among systematic uncertainties are to be expected, we will treat both datasets are uncorrelated.[28]

A constrained ($N^+ = N^0 = 3$) BCL fit using the same ansatz as for lattice-only data in Sec. 8.4, yields our average

$B \to D\ell\nu$ ($N_f = 2+1$)

	Central Values	Correlation Matrix					
$\|V_{cb}\|\times 10^3$	40.1 (1.0)	1	-0.525	-0.431	-0.185	-0.526	-0.497
a_0^+	0.8944 (95)	-0.525	1	0.282	-0.162	0.953	0.450
a_1^+	-8.08 (22)	-0.431	0.282	1	0.613	0.350	0.934
a_2^+	49.0 (4.6)	-0.185	-0.162	0.613	1	-0.0931	0.603
a_0^0	0.7802 (75)	-0.526	0.953	0.350	-0.0931	1	0.446
a_1^0	-3.42 (22)	-0.497	0.450	0.934	0.603	0.446	1

The fit is illustrated in Fig. 29. In passing, we note that, if correlations between the FNAL/MILC and HPQCD calculations are neglected, the V_{cb} central value rises to 40.3×10^{-3} in nice agreement with the results presented in Ref. [138].

Our results are summarized in Tab. 43, which also shows the HFAG inclusive determination of $|V_{cb}|$ for comparison, and illustrated in Fig. 30. The $N_f = 2+1$ results coming from $B \to D^*\ell\nu$ and $B \to D\ell\nu$ could in principle be averaged; we will however not do so, due to the difficulties of properly taking into account experimental correlations. We will thus leave them as separate exclusive estimates, which show good mutual consistence, and the well-known tension with the inclusive determination.

[27] We thank Marcello Rotondo for providing the ten bins result of the BaBar analysis.

[28] We have checked that results using just one experimental dataset are compatible within 1σ. In the case of BaBar, we have taken into account the introduction of some EW corrections in the data.

	from	$\lvert V_{cb}\rvert \times 10^3$
our average for $N_f = 2+1$	$B \to D^*\ell\nu$	39.27(56)(49)
our average for $N_f = 2+1$	$B \to D\ell\nu$	40.1(1.0)
our average for $N_f = 2$	$B \to D\ell\nu$	41.0(3.8)(1.5)
HFAG inclusive average	$B \to X_c\ell\nu$	42.46(88)

Table 43: Results for $|V_{cb}|$. When two errors are quoted in our averages, the first one comes from the lattice form factor, and the second from the experimental measurement. The HFAG inclusive average obtained in the kinetic scheme from Ref. [7] is shown for comparison.

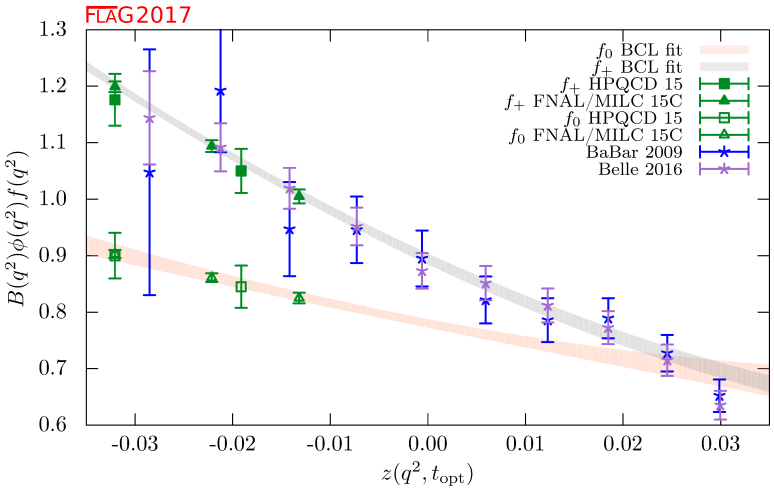

Figure 29: Lattice and experimental data for $f_+^{B\to D}(q^2)$ and $f_0^{B\to D}(q^2)$ versus z. Green symbols denote lattice-QCD points included in the fit, while blue and indigo points show experimental data divided by the value of $|V_{cb}|$ obtained from the fit. The grey and orange bands display the preferred $N^+ = N^0 = 3$ BCL fit (six parameters) to the lattice-QCD and experimental data with errors.

8.8 Nested averaging

At the web update of FLAG3 we encounter a case where the correlations among the results are much involved, namely the B meson bag parameters for $N_f = 2+1$, and a nested averaging scheme is required. In the following we describe the details of this scheme and how it is applied to the the $N_f = 2+1$ B meson bag parameters and their ratio.

Let us consider a quantity Q where an estimate from one collaboration is given by a ratio of two quantities: the numerator is of their own calculation but the denominator is a FLAG average or alike. Actually, in this particular case the denominator is a PDG [12] average, which is obtained using a procedure similar to that used by FLAG. Let us assign $i = 1$ for such an estimate, then

$$Q_1 = \frac{Y_1}{Z}. \tag{218}$$

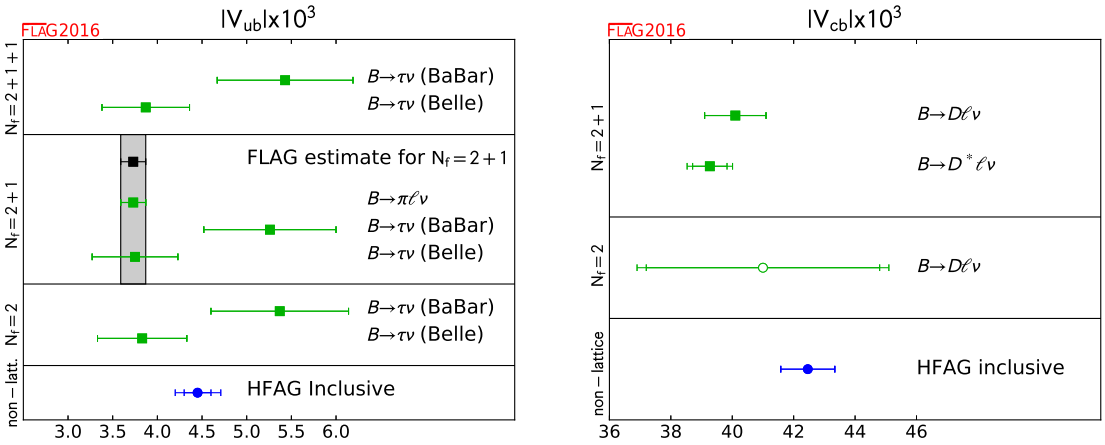

Figure 30: Left: Summary of $|V_{ub}|$ determined using: i) the B-meson leptonic decay branching fraction, $B(B^- \to \tau^- \bar{\nu})$, measured at the Belle and BaBar experiments, and our averages for f_B from lattice QCD; and ii) the various measurements of the $B \to \pi \ell \nu$ decay rates by Belle and BaBar, and our averages for lattice determinations of the relevant vector form factor $f_+(q^2)$. Right: Same for determinations of $|V_{cb}|$ using semileptonic decays. The HFAG inclusive results are from Ref. [7].

For the B meson bag parameter B_B as Q, $Y = B_B f_B^2$ and $Z = f_B^2$. The error of this result estimated by the authors is a simple error propagation from Y_1 and $\overline{Z}$. In principle Y_1 and $\overline{Z}$ have correlation, because $\overline{Z}$ is obtained with the results some of which have shared gauge field ensembles with the computation of Y_1 etc. But, they did not take the correlation into account, and we follow that. (For this special case it is likely that this procedure does not lead to underestimation of the error. See the next subsection for a discussion.) Let us make clear that we still need to take into account the correlation of other results Q_j $(j \geq 2)$ with Q_1 through $\overline{Z}$ if there is any. In our averaging procedure overlooking the correlation could lead to an underestimate of the error, while it is other way around for the error estimate of Q_1.

Now let us schematically write the error composition for Q_1,

$$Q_1 = \frac{Y_1}{\overline{Z}} = x_1 \pm \frac{\sigma^{(1)}_{Y_1}}{\overline{Z}} \pm \frac{\sigma^{(2)}_{Y_1}}{\overline{Z}} \pm \cdots \pm \frac{\sigma^{(E)}_{Y_1}}{\overline{Z}} \pm \frac{Y_1 \sigma_{\overline{Z}}}{\overline{Z}^2}, \tag{219}$$

where the last term represents the error propagating from $\overline{Z}$ and the others are ones form Y_1. Since we are considering the case where only one result is provided this way, the Q_j composition is same as Eq. (1) for the other results $(j \geq 2)$.

Now we would like to estimate the average and its error using Q_1, Q_2 $\cdots$ Q_M. As our average scheme does not take into account the correlations, we just need to follow a usual treatment for this case, too, where only central values and total errors enter. The error on the average needs a consideration as these data sets have an involved correlation among the errors. In the error composition in Eq. (219) $\sigma^{(\alpha)}_{Y_1}$ errors[29] can be treated in usual way. We

[29] Here we use Greek letters ((α) etc.) to label the different type of errors of a result, where previously (k) was used in Sec. 2.3. Italic letters (i, j, k etc.) are used to distinguishing different results.

consider cases where the average $\overline{Z}$ was obtained from results which have possible correlation with Q_j for $j \geq 2$. For the error estimate of the average of Q_i for $1 \leq i \leq M$ we need a *nested procedure* of FLAG averaging à la Schmelling.

The idea of Schmelling's scheme is to take into account the correlation among different "experiments" by introducing the degree of correlation between each pair of "experiments" (denoted by i and j) which is captured by the off-diagonal element of the correlation matrix C_{ij}, whose maximum is $C_{ij}^{\max} = \sqrt{C_{ii}C_{jj}}$. In the FLAG procedure an off-diagonal element is given by a partial sum of the decomposition of each C_{ii} and C_{jj} that are potentially correlated, which is expressed in Eq. (5). This procedure is easily extended in the situation discussed here, where we need to get into details of the error from $\overline{Z}$ (last term in Eq. (219)).

To proceed let us first write down the total error for each Q_i. The total error of Q_1, which we denote as σ_1, reads from Eq. (219)

$$\sigma_1^2 = \left(\frac{\sigma_{Y_1}^{(1)}}{\overline{Z}}\right)^2 + \left(\frac{\sigma_{Y_1}^{(2)}}{\overline{Z}}\right)^2 + \cdots + \left(\frac{\sigma_{Y_1}^{(E)}}{\overline{Z}}\right)^2 + \left(\frac{Y_1}{\overline{Z}^2}\right)^2 \sigma_{\overline{Z}}^2, \tag{220}$$

while the error of Q_j $(j \geq 2)$ is

$$\sigma_j^2 = \left(\sigma_j^{(1)}\right)^2 + \left(\sigma_j^{(2)}\right)^2 + \cdots + \left(\sigma_j^{(E)}\right)^2. \tag{221}$$

Correlation between Q_j and Q_k $(j, k \geq 2)$ is taken care of by usual method, where we need to find the correlated elements in $\sigma_j^{(\alpha)}$. The correlated elements between Q_1 and Q_j $(j \geq 2)$ can be similarly found. For that we need to recall $\sigma_{\overline{Z}}$ is given from Eq. (7) as

$$\sigma_{\overline{Z}}^2 = \sum_{i',j'=1}^{M'} \omega[Z]_{i'}\omega[Z]_{j'}C[Z]_{i'j'}. \tag{222}$$

Here we explicitly noted Z for each quantity for clarity. The indices i' and j' run over to M' which is in general different from M for Q.

To construct the correlation matrix C_{ij} of Q_i we need σ_i for the diagonal elements, that we already know, and $\sigma_{i;j}$ which goes into the off-diagonal elements. $\sigma_{i;j}$ for $i,\ j \geq 2$ are defined in the usual way, Eq. (5). For $\sigma_{1;k}$ $(k \geq 2)$ we take

$$\sigma_{1;k} = \sqrt{\frac{1}{\overline{Z}^2}{\sum_{(\alpha)\leftrightarrow k}}' \left[\sigma_{Y_1}^{(\alpha)}\right]^2 + \frac{Y_1^2}{\overline{Z}^4}\sum_{i',j'}^{M'} \omega[Z]_{i'}\omega[Z]_{j'}C[Z]_{i'j'\leftrightarrow k}}\ . \tag{223}$$

In the first term a new notation is introduced for the summation to clearly indicate that it is taken over only $\sigma_{Y_1}^{(\alpha)}$ which has correlation with Q_k. In the second term $C[Z]_{i'j'\leftrightarrow k}$ is defined with $\sigma[Z]_{i'\leftrightarrow k}$ and $\sigma[Z]_{i';j'\leftrightarrow k}$, both of which are defined with summation over subsets of $(\sigma[Z]_{i'}^{(\alpha)})^2$, like

$$C[Z]_{i'i'\leftrightarrow k} = (\sigma[Z]_{i'\leftrightarrow k})^2 \qquad (i' = 1, \cdots, M')\ , \tag{224}$$

$$(\sigma[Z]_{i'\leftrightarrow k})^2 = {\sum_{(\alpha)\leftrightarrow k}}' (\sigma[Z]_{i'}^{(\alpha)})^2, \tag{225}$$

where the summation $\sum'_{(\alpha)\leftrightarrow k}$ over (α) is restricted to $\sigma[Z]^{(\alpha)}_{i'}$ that have correlation with Q_k, and

$$C[Z]_{i'j'\leftrightarrow k} = \sigma[Z]_{i';j'\leftrightarrow k}\,\sigma[Z]_{j';i'\leftrightarrow k} \qquad (i' \neq j') \ , \tag{226}$$

$$\sigma[Z]_{i';j'\leftrightarrow k} = \sqrt{\sum_{(\alpha)\leftrightarrow j'k}{}' (\sigma[Z]^{(\alpha)}_{i'})^2}, \tag{227}$$

where the summation $\sum'_{(\alpha)\leftrightarrow j'k}$ over (α) is restricted to $\sigma[Z]^{(\alpha)}_{i'}$ that have correlation with *both* $Z_{j'}$ and Q_k. Finally the last quantity that we need to define is $\sigma_{k;1}$.

$$\sigma_{k;1} = \sqrt{\sum_{(\alpha)\leftrightarrow 1}{}' \left[\sigma^{(\alpha)}_k\right]^2} \ , \tag{228}$$

where the summation $\sum'_{(\alpha)\leftrightarrow 1}$ should be restricted to $\sigma^{(\alpha)}_k$ that have correlation with one of the terms in Eq. (220).

8.8.1 A note on error propagation

Let us consider a slightly different ratio than Eq. (218)

$$Q'_1 = \tfrac{Y_1}{Z_1}, \tag{229}$$

as a gedanken experiment where Z_1 from the same calculation set-up existed. The collaboration have not calculated Z_1 yet, that is the reason why they used the "world average" $\overline{Z}$. If one takes into account the correlation among Y_1 and Z_1 then the error tends to cancel and get smaller than the error estimated from the simple error propagation. Thus, the simple propagating error overestimates the true error in this case. Note that this is not a general statement and only applied for certain quantities. In case of Eq. (218), Y_1 is correlated in some, but not all results that enter the average $\overline{Z}$. Thus the simple propagating error will work better than in the case of Eq. (229) and will not underestimate the true error.

References

[1] LHCb, CMS collaboration, V. Khachatryan et al., *Observation of the rare $B_s^0 \to \mu^+\mu^-$ decay from the combined analysis of CMS and LHCb data*, *Nature* **522** (2015) 68–72, [1411.4413].

[2] J. L. Rosner, S. Stone and R. S. Van de Water, *Leptonic Decays of Charged Pseudoscalar Mesons, in Review of Particle Physics [52] 2015 update*, 1509.02220.

[3] BABAR collaboration, J. Lees et al., *Evidence of $B \to \tau\nu$ decays with hadronic B tags*, *Phys.Rev.* **D88** (2013) 031102, [1207.0698].

[4] BELLE collaboration, B. Kronenbitter et al., *Measurement of the branching fraction of $B^+ \to \tau^+\nu_\tau$ decays with the semileptonic tagging method*, *Phys. Rev.* **D92** (2015) 051102, [1503.05613].

[5] C. Bobeth, M. Gorbahn, T. Hermann, M. Misiak, E. Stamou and M. Steinhauser, *$B_{s,d} \to l^+l^-$ in the Standard Model with Reduced Theoretical Uncertainty*, *Phys. Rev. Lett.* **112** (2014) 101801, [1311.0903].

[6] K. De Bruyn, R. Fleischer, R. Knegjens, P. Koppenburg, M. Merk and N. Tuning, *Branching Ratio Measurements of B_s Decays*, *Phys. Rev.* **D86** (2012) 014027, [1204.1735].

[7] [HFAG 14] Y. Amhis et al., *Averages of b-hadron, c-hadron, and τ-lepton properties as of summer 2014*, 1412.7515.

[8] LHCb collaboration, R. Aaij et al., *Precision measurement of CP violation in $B_s^0 \to J/\psi K^+K^-$ decays*, *Phys. Rev. Lett.* **114** (2015) 041801, [1411.3104].

[9] [ETM 13B] N. Carrasco et al., *B-physics from $N_f = 2$ tmQCD: the Standard Model and beyond*, *JHEP* **1403** (2014) 016, [1308.1851].

[10] [HPQCD 12] H. Na, C. J. Monahan, C. T. Davies, R. Horgan, G. P. Lepage et al., *The B and B_s meson decay constants from lattice QCD*, *Phys.Rev.* **D86** (2012) 034506, [1202.4914].

[11] [FLAG 13] S. Aoki, Y. Aoki, C. Bernard, T. Blum, G. Colangelo et al., *Review of lattice results concerning low-energy particle physics*, *Eur.Phys.J.* **C74** (2014) 2890, [1310.8555].

[12] [ETM 13E] N. Carrasco, P. Dimopoulos, R. Frezzotti, V. Giménez, P. Lami et al., *A $N_f = 2+1+1$ 'twisted' determination of the b-quark mass, f_B and f_{B_s}*, *PoS* **LATTICE2013** (2014) 313, [1311.2837].

[13] [HPQCD 13] R. J. Dowdall, C. Davies, R. Horgan, C. Monahan and J. Shigemitsu, *B-meson decay constants from improved lattice NRQCD and physical u, d, s and c sea quarks*, *Phys.Rev.Lett.* **110** (2013) 222003, [1302.2644].

[14] [RBC/UKQCD 14] N. H. Christ, J. M. Flynn, T. Izubuchi, T. Kawanai, C. Lehner et al., *B-meson decay constants from 2+1-flavor lattice QCD with domain-wall light quarks and relativistic heavy quarks*, *Phys.Rev.* **D91** (2015) 054502, [1404.4670].

[15] [RBC/UKQCD 14A] Y. Aoki, T. Ishikawa, T. Izubuchi, C. Lehner and A. Soni, *Neutral B meson mixings and B meson decay constants with static heavy and domain-wall light quarks*, *Phys. Rev.* **D91** (2015) 114505, [1406.6192].

[16] [RBC/UKQCD 13A] O. Witzel, *B-meson decay constants with domain-wall light quarks and nonperturbatively tuned relativistic b-quarks*, *PoS* **LATTICE2013** (2014) 377, [1311.0276].

[17] [HPQCD 11A] C. McNeile, C. T. H. Davies, E. Follana, K. Hornbostel and G. P. Lepage, *High-precision f_{B_s} and HQET from relativistic lattice QCD*, *Phys.Rev.* **D85** (2012) 031503, [1110.4510].

[18] [FNAL/MILC 11] A. Bazavov et al., *B- and D-meson decay constants from three-flavor lattice QCD*, *Phys.Rev.* **D85** (2012) 114506, [1112.3051].

[19] [HPQCD 09] E. Gamiz, C. T. Davies, G. P. Lepage, J. Shigemitsu and M. Wingate, *Neutral B meson mixing in unquenched lattice QCD*, *Phys.Rev.* **D80** (2009) 014503, [0902.1815].

[20] [ALPHA 14] F. Bernardoni et al., *Decay constants of B-mesons from non-perturbative HQET with two light dynamical quarks*, *Phys.Lett.* **B735** (2014) 349–356, [1404.3590].

[21] [ALPHA 13] F. Bernardoni, B. Blossier, J. Bulava, M. Della Morte, P. Fritzsch et al., *B-physics with $N_f = 2$ Wilson fermions*, *PoS* **LATTICE2013** (2014) 381, [1309.1074].

[22] [ETM 13C] N. Carrasco et al., *B-physics computations from Nf=2 tmQCD*, *PoS* **LATTICE2013** (2014) 382, [1310.1851].

[23] [ALPHA 12A] F. Bernardoni, B. Blossier, J. Bulava, M. Della Morte, P. Fritzsch et al., *B-physics from HQET in two-flavour lattice QCD*, *PoS* **LAT2012** (2012) 273, [1210.7932].

[24] [ETM 12B] N. Carrasco, P. Dimopoulos, R. Frezzotti, V. Gimenez, G. Herdoiza et al., *B-physics from the ratio method with Wilson twisted mass fermions*, *PoS* **LAT2012** (2012) 104, [1211.0568].

[25] [ALPHA 11] B. Blossier, J. Bulava, M. Della Morte, M. Donnellan, P. Fritzsch et al., *M_b and f_B from non-perturbatively renormalized HQET with $N_f = 2$ light quarks*, *PoS* **LAT2011** (2011) 280, [1112.6175].

[26] [ETM 11A] P. Dimopoulos et al., *Lattice QCD determination of m_b, f_B and f_{B_s} with twisted mass Wilson fermions*, *JHEP* **1201** (2012) 046, [1107.1441].

[27] [ETM 09D] B. Blossier et al., *A proposal for B-physics on current lattices*, *JHEP* **1004** (2010) 049, [0909.3187].

[28] [HPQCD 05B] A. Gray et al., *The upsilon spectrum and m_b from full lattice QCD*, *Phys.Rev.* **D72** (2005) 094507, [hep-lat/0507013].

[29] [RBC/UKQCD 10C] C. Albertus et al., *Neutral B-meson mixing from unquenched lattice QCD with domain-wall light quarks and static b-quarks*, *Phys.Rev.* **D82** (2010) 014505, [1001.2023].

[30] M. Lüscher, *Solution of the Dirac equation in lattice QCD using a domain decomposition method*, *Comput. Phys. Commun.* **156** (2004) 209–220, [hep-lat/0310048].

[31] M. Lüscher, *Schwarz-preconditioned HMC algorithm for two-flavour lattice QCD*, *Comput. Phys. Commun.* **165** (2005) 199–220, [hep-lat/0409106].

[32] M. Lüscher, *Deflation acceleration of lattice QCD simulations*, *JHEP* **12** (2007) 011, [0710.5417].

[33] M. Marinkovic and S. Schaefer, *Comparison of the mass preconditioned HMC and the DD-HMC algorithm for two-flavour QCD*, *PoS* **LATTICE2010** (2010) 031, [1011.0911].

[34] D. Arndt and C. J. D. Lin, *Heavy meson chiral perturbation theory in finite volume*, *Phys. Rev.* **D70** (2004) 014503, [hep-lat/0403012].

[35] [ALPHA 03] J. Heitger and R. Sommer, *Nonperturbative heavy quark effective theory*, *JHEP* **0402** (2004) 022, [hep-lat/0310035].

[36] M. Della Morte, N. Garron, M. Papinutto and R. Sommer, *Heavy quark effective theory computation of the mass of the bottom quark*, *JHEP* **01** (2007) 007, [hep-ph/0609294].

[37] [ALPHA 10B] B. Blossier, M. Della Morte, N. Garron and R. Sommer, *HQET at order $1/m$: I. Non-perturbative parameters in the quenched approximation*, *JHEP* **1006** (2010) 002, [1001.4783].

[38] [ALPHA 12D] B. Blossier et al., *Parameters of heavy quark effective theory from $N_f = 2$ lattice QCD*, *JHEP* **1209** (2012) 132, [1203.6516].

[39] [ALPHA 13C] F. Bernardoni et al., *The b-quark mass from non-perturbative $N_f = 2$ Heavy Quark Effective Theory at $O(1/m_h)$*, *Phys. Lett.* **B730** (2014) 171–177, [1311.5498].

[40] [ALPHA 12] P. Fritzsch, F. Knechtli, B. Leder, M. Marinkovic, S. Schaefer et al., *The strange quark mass and the Λ parameter of two flavor QCD*, *Nucl.Phys.* **B865** (2012) 397–429, [1205.5380].

[41] B. Blossier, M. Della Morte, G. von Hippel, T. Mendes and R. Sommer, *On the generalized eigenvalue method for energies and matrix elements in lattice field theory*, *JHEP* **04** (2009) 094, [0902.1265].

[42] [RBC/UKQCD 10A] Y. Aoki et al., *Continuum limit physics from 2+1 flavor domain wall QCD*, *Phys.Rev.* **D83** (2011) 074508, [1011.0892].

[43] [RBC/UKQCD 08] C. Allton et al., *Physical results from 2+1 flavor domain wall QCD and SU(2) chiral perturbation theory*, *Phys. Rev.* **D78** (2008) 114509, [0804.0473].

[44] N. H. Christ, M. Li and H.-W. Lin, *Relativistic heavy quark effective action*, *Phys.Rev.* **D76** (2007) 074505, [hep-lat/0608006].

[45] [RBC/UKQCD 12A] Y. Aoki et al., *Nonperturbative tuning of an improved relativistic heavy-quark action with application to bottom spectroscopy*, *Phys.Rev.* **D86** (2012) 116003, [1206.2554].

[46] A. X. El-Khadra, A. S. Kronfeld, P. B. Mackenzie, S. M. Ryan and J. N. Simone, *The semileptonic decays $B \to \pi\ell\nu$ and $D \to \pi\ell\nu$ from lattice QCD*, *Phys.Rev.* **D64** (2001) 014502, [hep-ph/0101023].

[47] A. Hasenfratz and F. Knechtli, *Flavor symmetry and the static potential with hypercubic blocking*, *Phys.Rev.* **D64** (2001) 034504, [hep-lat/0103029].

[48] [FNAL/MILC 15A] A. Bazavov et al., *Decay Constants f_B and f_{B_s} from HISQ Simulations*, *PoS* **LATTICE2015** (2016) 331, [1511.02294].

[49] A. Walker-Loud, *Strong isospin breaking with twisted mass lattice QCD*, 0904.2404.

[50] T. Inami and C. S. Lim, *Effects of superheavy quarks and leptons in low-energy weak processes $K_L \to \mu\bar{\mu}$, $K^+ \to \pi^+\nu\bar{\nu}$ and $K^0 \leftrightarrow \bar{K}^0$*, *Prog. Theor. Phys.* **65** (1981) 297.

[51] G. Buchalla, A. J. Buras and M. E. Lautenbacher, *Weak decays beyond leading logarithms*, *Rev. Mod. Phys.* **68** (1996) 1125–1144, [hep-ph/9512380].

[52] Particle Data Group collaboration, K. A. Olive et al., *Review of Particle Physics*, *Chin. Phys.* **C38** (2014) 090001 and 2015 update.

[53] F. Gabbiani, E. Gabrielli, A. Masiero and L. Silvestrini, *A Complete analysis of FCNC and CP constraints in general SUSY extensions of the standard model*, *Nucl. Phys.* **B477** (1996) 321–352, [hep-ph/9604387].

[54] A. Lenz and U. Nierste, *Theoretical update of $B_s - \bar{B}_s$ mixing*, *JHEP* **0706** (2007) 072, [hep-ph/0612167].

[55] M. Beneke, G. Buchalla and I. Dunietz, *Width difference in the $B_s - \bar{B}_s$ system*, *Phys.Rev.* **D54** (1996) 4419–4431, [hep-ph/9605259].

[56] [FNAL/MILC 11A] C. M. Bouchard, E. Freeland, C. Bernard, A. El-Khadra, E. Gamiz et al., *Neutral B mixing from $2+1$ flavor lattice-QCD: the Standard Model and beyond*, *PoS* **LAT2011** (2011) 274, [1112.5642].

[57] [FNAL/MILC 16] A. Bazavov et al., *$B^0_{(s)}$-mixing matrix elements from lattice QCD for the Standard Model and beyond*, *Phys. Rev.* **D93** (2016) 113016, [1602.03560].

[58] [HPQCD 06A] E. Dalgic, A. Gray, E. Gamiz, C. T. Davies, G. P. Lepage et al., *$B^0_s - \bar{B}^0_s$ mixing parameters from unquenched lattice QCD*, *Phys.Rev.* **D76** (2007) 011501, [hep-lat/0610104].

[59] [ETM 12A] N. Carrasco et al., *Neutral meson oscillations in the Standard Model and beyond from $N_f = 2$ twisted mass lattice QCD*, *PoS* **LAT2012** (2012) 105, [1211.0565].

[60] [FNAL/MILC 12] A. Bazavov, C. Bernard, C. Bouchard, C. DeTar, M. Di Pierro et al., *Neutral B-meson mixing from three-flavor lattice QCD: determination of the SU(3)-breaking ratio ξ*, *Phys.Rev.* **D86** (2012) 034503, [1205.7013].

[61] [ALPHA 05A] M. Della Morte, A. Shindler and R. Sommer, *On lattice actions for static quarks*, *JHEP* **0508** (2005) 051, [hep-lat/0506008].

[62] [MILC 13B] C. Bernard, *Neutral B mixing in staggered chiral perturbation theory*, *Phys.Rev.* **D87** (2013) 114503, [1303.0435].

[63] M. Della Morte, B. Jäger, T. Rae and H. Wittig, *Improved interpolating fields for hadrons at non-zero momentum*, *Eur.Phys.J.* **A48** (2012) 139, [1208.0189].

[64] D. Bećirević and A. B. Kaidalov, *Comment on the heavy → light form-factors*, *Phys.Lett.* **B478** (2000) 417–423, [hep-ph/9904490].

[65] P. Ball and R. Zwicky, *New results on $B \to \pi, K, \eta$ decay form factors from light-cone sum rules*, *Phys.Rev.* **D71** (2005) 014015, [hep-ph/0406232].

[66] D. Becirevic, A. L. Yaouanc, A. Oyanguren, P. Roudeau and F. Sanfilippo, *Insight into $D/B \to \pi\ell\nu_\ell$ decay using the pole models*, 1407.1019.

[67] R. J. Hill, *Heavy-to-light meson form-factors at large recoil*, *Phys.Rev.* **D73** (2006) 014012, [hep-ph/0505129].

[68] G. P. Lepage and S. J. Brodsky, *Exclusive processes in perturbative Quantum Chromodynamics*, *Phys.Rev.* **D22** (1980) 2157.

[69] R. Akhoury, G. F. Sterman and Y. Yao, *Exclusive semileptonic decays of B mesons into light mesons*, *Phys.Rev.* **D50** (1994) 358–372.

[70] L. Lellouch, *Lattice constrained unitarity bounds for $\bar{B}^0 \to \pi^+ \ell\, \bar{\nu}_l$ decays*, *Nucl.Phys.* **B479** (1996) 353–391, [hep-ph/9509358].

[71] C. Bourrely, I. Caprini and L. Lellouch, *Model-independent description of $B \to \pi\ell\nu$ decays and a determination of $|V_{ub}|$*, *Phys.Rev.* **D79** (2009) 013008, [0807.2722].

[72] C. Bourrely, B. Machet and E. de Rafael, *Semileptonic decays of pseudoscalar particles ($M \to M'\ell\nu_\ell$) and short distance behavior of Quantum Chromodynamics*, *Nucl. Phys.* **B189** (1981) 157.

[73] C. G. Boyd, B. Grinstein and R. F. Lebed, *Constraints on form-factors for exclusive semileptonic heavy to light meson decays*, *Phys.Rev.Lett.* **74** (1995) 4603–4606, [hep-ph/9412324].

[74] C. G. Boyd and M. J. Savage, *Analyticity, shapes of semileptonic form-factors, and $\bar{B} \to \pi\ell\bar{\nu}$*, *Phys.Rev.* **D56** (1997) 303–311, [hep-ph/9702300].

[75] M. C. Arnesen, B. Grinstein, I. Z. Rothstein and I. W. Stewart, *A precision model independent determination of $|V_{ub}|$ from $B \to \pi e\nu$*, *Phys.Rev.Lett.* **95** (2005) 071802, [hep-ph/0504209].

[76] T. Becher and R. J. Hill, *Comment on form-factor shape and extraction of $|V_{ub}|$ from $B \to \pi l\nu$*, *Phys.Lett.* **B633** (2006) 61–69, [hep-ph/0509090].

[77] R. J. Hill, *The Modern description of semileptonic meson form factors*, *eConf* **C060409** (2006) 027, [hep-ph/0606023].

[78] R. J. Hill and G. Paz, *Model independent extraction of the proton charge radius from electron scattering*, *Phys. Rev.* **D82** (2010) 113005, [1008.4619].

[79] R. J. Hill and G. Paz, *Model independent analysis of proton structure for hydrogenic bound states*, *Phys. Rev. Lett.* **107** (2011) 160402, [1103.4617].

[80] Z. Epstein, G. Paz and J. Roy, *Model independent extraction of the proton magnetic radius from electron scattering*, *Phys. Rev.* **D90** (2014) 074027, [1407.5683].

[81] [HPQCD 06] E. Dalgic et al., *B meson semileptonic form-factors from unquenched lattice QCD*, *Phys.Rev.* **D73** (2006) 074502, [hep-lat/0601021].

[82] [FNAL/MILC 08A] J. A. Bailey et al., *The $B \to \pi\ell\nu$ semileptonic form factor from three-flavor lattice QCD: a model-independent determination of $|V_{ub}|$*, *Phys.Rev.* **D79** (2009) 054507, [0811.3640].

[83] [FNAL/MILC 15] J. A. Bailey et al., *$|V_{ub}|$ from $B \to \pi\ell\nu$ decays and (2+1)-flavor lattice QCD*, *Phys. Rev.* **D92** (2015) 014024, [1503.07839].

[84] [RBC/UKQCD 15] J. M. Flynn, T. Izubuchi, T. Kawanai, C. Lehner, A. Soni, R. S. Van de Water et al., *$B \to \pi\ell\nu$ and $B_s \to K\ell\nu$ form factors and $|V_{ub}|$ from 2+1-flavor lattice QCD with domain-wall light quarks and relativistic heavy quarks*, *Phys. Rev.* **D91** (2015) 074510, [1501.05373].

[85] [HPQCD 15A] B. Colquhoun, R. J. Dowdall, J. Koponen, C. T. H. Davies and G. P. Lepage, *$B \to \pi\ell\nu$ at zero recoil from lattice QCD with physical u/d quarks*, *Phys. Rev.* **D93** (2016) 034502, [1510.07446].

[86] [HPQCD 12C] C. M. Bouchard, G. P. Lepage, C. J. Monahan, H. Na and J. Shigemitsu, *Form factors for B and B_s semileptonic decays with NRQCD/HISQ quarks*, *PoS* **LAT2012** (2012) 118, [1210.6992].

[87] [HPQCD 13F] C. M. Bouchard, G. P. Lepage, J. C. Monahan, H. Na and J. Shigemitsu, *B and B_s semileptonic decay form factors with NRQCD/HISQ quarks*, *PoS* **LATTICE2013** (2014) 387, [1310.3207].

[88] J. Bijnens and I. Jemos, *Hard Pion Chiral Perturbation Theory for $B \to \pi$ and $D \to \pi$ Formfactors*, *Nucl. Phys.* **B840** (2010) 54–66, [1006.1197].

[89] M. Procura, G. Colangelo, L. Rothen, R. Stucki and J. Tarrús Castellà, *A scrutiny of hard pion chiral perturbation theory*, *PoS* **CD12** (2013) 049.

[90] [HPQCD 14] C. M. Bouchard, G. P. Lepage, C. Monahan, H. Na and J. Shigemitsu, *$B_s \to K\ell\nu$ form factors from lattice QCD*, *Phys. Rev.* **D90** (2014) 054506, [1406.2279].

[91] [ALPHA 14B] F. Bahr, F. Bernardoni, J. Bulava, A. Joseph, A. Ramos, H. Simma et al., *Form factors for $\mathrm{B_s} \to \mathrm{K}\ell\nu$ decays in Lattice QCD*, in *8th International Workshop on the CKM Unitarity Triangle (CKM2014) Vienna, Austria, September 8-12, 2014*, 2014. 1411.3916.

[92] M. Antonelli et al., *Flavor physics in the quark sector*, *Phys.Rept.* **494** (2010) 197–414, [0907.5386].

[93] Z. Liu et al., *Form factors for rare B decays: strategy, methodology, and numerical study*, *PoS* **LAT2009** (2009) 242, [0911.2370].

[94] [HPQCD 13E] C. Bouchard, G. P. Lepage, C. Monahan, H. Na and J. Shigemitsu, *Rare decay $B \to K\ell^+\ell^-$ form factors from lattice QCD*, *Phys. Rev.* **D88** (2013) 054509, [1306.2384].

[95] [FNAL/MILC 15D] J. A. Bailey et al., *$B \to Kl^+l^-$ decay form factors from three-flavor lattice QCD*, *Phys. Rev.* **D93** (2016) 025026, [1509.06235].

[96] [FNAL/MILC 15E] J. A. Bailey et al., *$B \to \pi\ell\ell$ form factors for new-physics searches from lattice QCD*, *Phys. Rev. Lett.* **115** (2015) 152002, [1507.01618].

[97] [HPQCD 13D] C. Bouchard, G. P. Lepage, C. Monahan, H. Na and J. Shigemitsu, *Standard Model predictions for $B \to Kll$ with form factors from lattice QCD*, *Phys. Rev. Lett.* **111** (2013) 162002, [1306.0434].

[98] [FNAL/MILC 15F] D. Du, A. X. El-Khadra, S. Gottlieb, A. S. Kronfeld, J. Laiho, E. Lunghi et al., *Phenomenology of semileptonic B-meson decays with form factors from lattice QCD*, *Phys. Rev.* **D93** (2016) 034005, [1510.02349].

[99] C. B. Lang, D. Mohler, S. Prelovsek and R. M. Woloshyn, *Predicting positive parity B_s mesons from lattice QCD*, *Phys. Lett.* **B750** (2015) 17–21, [1501.01646].

[100] M. Lüscher, *Volume Dependence of the Energy Spectrum in Massive Quantum Field Theories. 2. Scattering States*, *Commun. Math. Phys.* **105** (1986) 153–188.

[101] M. Lüscher, *Two particle states on a torus and their relation to the scattering matrix*, *Nucl. Phys.* **B354** (1991) 531–578.

[102] M. Lüscher, *Signatures of unstable particles in finite volume*, *Nucl. Phys.* **B364** (1991) 237–254.

[103] M. Lage, U.-G. Meissner and A. Rusetsky, *A Method to measure the antikaon-nucleon scattering length in lattice QCD*, *Phys. Lett.* **B681** (2009) 439–443, [0905.0069].

[104] V. Bernard, M. Lage, U. G. Meissner and A. Rusetsky, *Scalar mesons in a finite volume*, *JHEP* **01** (2011) 019, [1010.6018].

[105] M. Doring, U.-G. Meissner, E. Oset and A. Rusetsky, *Unitarized Chiral Perturbation Theory in a finite volume: Scalar meson sector*, *Eur. Phys. J.* **A47** (2011) 139, [1107.3988].

[106] M. T. Hansen and S. R. Sharpe, *Multiple-channel generalization of Lellouch-Luscher formula*, *Phys. Rev.* **D86** (2012) 016007, [1204.0826].

[107] R. A. Briceno and Z. Davoudi, *Moving multichannel systems in a finite volume with application to proton-proton fusion*, *Phys. Rev.* **D88** (2013) 094507, [1204.1110].

[108] [HS 14] J. J. Dudek, R. G. Edwards, C. E. Thomas and D. J. Wilson, *Resonances in coupled $\pi K - \eta K$ scattering from quantum chromodynamics*, *Phys. Rev. Lett.* **113** (2014) 182001, [1406.4158].

[109] R. R. Horgan, Z. Liu, S. Meinel and M. Wingate, *Lattice QCD calculation of form factors describing the rare decays $B \to K^* \ell^+ \ell^-$ and $B_s \to \phi \ell^+ \ell^-$*, *Phys. Rev.* **D89** (2014) 094501, [1310.3722].

[110] R. R. Horgan, Z. Liu, S. Meinel and M. Wingate, *Calculation of $B^0 \to K^{*0} \mu^+ \mu^-$ and $B_s^0 \to \phi \mu^+ \mu^-$ observables using form factors from lattice QCD*, *Phys. Rev. Lett.* **112** (2014) 212003, [1310.3887].

[111] [RBC/UKQCD 15B] J. Flynn, A. Jüttner, T. Kawanai, E. Lizarazo and O. Witzel, *Hadronic form factors for rare semileptonic B decays*, in *Proceedings, 33rd International Symposium on Lattice Field Theory (Lattice 2015)*, vol. LATTICE2015, p. 345, 2016. 1511.06622.

[112] A. Sirlin, *Large m_W, m_Z behavior of the $O(\alpha)$ corrections to semileptonic processes mediated by W*, *Nucl.Phys.* **B196** (1982) 83.

[113] M. E. Luke, *Effects of subleading operators in the heavy quark effective theory*, *Phys. Lett.* **B252** (1990) 447–455.

[114] [FNAL/MILC 04A] M. Okamoto et al., *Semileptonic $D \to \pi/K$ and $B \to \pi/D$ decays in 2+1 flavor lattice QCD*, *Nucl.Phys.Proc.Suppl.* **140** (2005) 461–463, [hep-lat/0409116].

[115] [FNAL/MILC 13B] S.-W. Qiu , C. DeTar, A. X. El-Khadra, A. S. Kronfeld, J. Laiho et al., *Semileptonic decays $B \to D^{(*)} l \nu$ at nonzero recoil*, *PoS* **LATTICE2013** (2014) 385, [1312.0155].

[116] M. Atoui, V. Morenas, D. Becirevic and F. Sanfilippo, *$b_s \to d_s \ell \nu_\ell$ near zero recoil in and beyond the standard model*, *Eur. Phys. J.* **C74** (2014) 2861, [1310.5238].

[117] [FNAL/MILC 08] C. Bernard et al., *The $\bar{B} \to D^* \ell \bar{\nu}$ form factor at zero recoil from three-flavor lattice QCD: a model independent determination of $|V_{cb}|$*, *Phys.Rev.* **D79** (2009) 014506, [0808.2519].

[118] [FNAL/MILC 14] J. A. Bailey et al., *Update of $|V_{cb}|$ from the $\bar{B} \to D^* \ell \bar{\nu}$ form factor at zero recoil with three-flavor lattice QCD*, *Phys. Rev.* **D89** (2014) 114504, [1403.0635].

[119] [FNAL/MILC 15C] J. A. Bailey et al., *BD form factors at nonzero recoil and $-V_{cb}-$ from 2+1-flavor lattice QCD*, *Phys. Rev.* **D92** (2015) 034506, [1503.07237].

[120] [HPQCD 15] H. Na, C. M. Bouchard, G. P. Lepage, C. Monahan and J. Shigemitsu, *BDl form factors at nonzero recoil and extraction of $-V_{cb}-$*, *Phys. Rev.* **D92** (2015) 054510, [1505.03925].

[121] [ETM 10B] B. Blossier et al., *Average up/down, strange and charm quark masses with $N_f = 2$ twisted mass lattice QCD*, *Phys. Rev.* **D82** (2010) 114513, [1010.3659].

[122] [FNAL/MILC 12C] J. A. Bailey et al., *$B_s \to D_s/B \to D$ semileptonic form-factor ratios and their application to $BR(B_s^0 \to \mu^+\mu^-)$*, *Phys.Rev.* **D85** (2012) 114502, [1202.6346].

[123] LHCb collaboration, R. Aaij et al., *Determination of f_s/f_d for 7 TeV pp collisions and a measurement of the branching fraction of the decay $B_d \to D^- K^+$*, *Phys. Rev. Lett.* **107** (2011) 211801, [1106.4435].

[124] L. Randall and M. B. Wise, *Chiral perturbation theory for $B \to D^*$ and $B \to D$ semileptonic transition matrix elements at zero recoil*, *Phys.Lett.* **B303** (1993) 135–139, [hep-ph/9212315].

[125] M. J. Savage, *Heavy meson observables at one loop in partially quenched chiral perturbation theory*, *Phys.Rev.* **D65** (2002) 034014, [hep-ph/0109190].

[126] S. Hashimoto, A. S. Kronfeld, P. B. Mackenzie, S. M. Ryan and J. N. Simone, *Lattice calculation of the zero recoil form-factor of $\bar{B} \to D^* \ell \bar{\nu}$: toward a model independent determination of $|V_{cb}|$*, *Phys.Rev.* **D66** (2002) 014503, [hep-ph/0110253].

[127] W. Detmold, C. Lehner and S. Meinel, *$\Lambda_b \to p\ell^-\bar{\nu}_\ell$ and $\Lambda_b \to \Lambda_c \ell^- \bar{\nu}_\ell$ form factors from lattice QCD with relativistic heavy quarks*, *Phys. Rev.* **D92** (2015) 034503, [1503.01421].

[128] LHCb collaboration, R. Aaij et al., *Determination of the quark coupling strength $|V_{ub}|$ using baryonic decays*, *Nature Phys.* **11** (2015) 743–747, [1504.01568].

[129] T. Feldmann and M. W. Y. Yip, *Form Factors for Lambda$_b \to \Lambda$ Transitions in SCET*, *Phys. Rev.* **D85** (2012) 014035, [1111.1844].

[130] Belle collaboration, I. Adachi et al., *Measurement of $B^- \to \tau^- \bar{\nu}_\tau$ with a hadronic tagging method using the full data sample of Belle*, *Phys. Rev. Lett.* **110** (2013) 131801, [1208.4678].

[131] BABAR collaboration, B. Aubert et al., *A search for $B^+ \to \ell^+ \nu_\ell$ recoiling against $B^- \to D^0 \ell^- \bar{\nu} X$*, *Phys.Rev.* **D81** (2010) 051101, [0912.2453].

[132] BABAR collaboration, P. del Amo Sanchez et al., *Study of $B \to \pi \ell \nu$ and $B \to \rho \ell \nu$ Decays and Determination of $|V_{ub}|$*, *Phys.Rev.* **D83** (2011) 032007, [1005.3288].

[133] BABAR collaboration, J. Lees et al., *Branching fraction and form-factor shape measurements of exclusive charmless semileptonic B decays, and determination of $|V_{ub}|$*, *Phys.Rev.* **D86** (2012) 092004, [1208.1253].

[134] Belle collaboration, H. Ha et al., *Measurement of the decay $B^0 \to \pi^- \ell^+ \nu$ and determination of $|V_{ub}|$*, *Phys.Rev.* **D83** (2011) 071101, [1012.0090].

[135] Belle collaboration, A. Sibidanov et al., *Study of Exclusive $B \to X_u \ell \nu$ Decays and Extraction of $\|V_{ub}\|$ using Full Reconstruction Tagging at the Belle Experiment*, *Phys. Rev.* **D88** (2013) 032005, [1306.2781].

[136] Belle collaboration, R. Glattauer et al., *Measurement of the decay $B \to D \ell \nu_\ell$ in fully reconstructed events and determination of the Cabibbo-Kobayashi-Maskawa matrix element $|V_{cb}|$*, *Phys. Rev.* **D93** (2016) 032006, [1510.03657].

[137] BaBar collaboration, B. Aubert et al., *Measurement of $|V(cb)|$ and the Form-Factor Slope in $\overline{B} \to D\ell^{-}\overline{\nu}_{\ell}$ Decays in Events Tagged by a Fully Reconstructed B Meson*, *Phys. Rev. Lett.* **104** (2010) 011802, [0904.4063].

[138] D. Bigi and P. Gambino, *Revisiting $B \to D\ell\nu$*, *Phys. Rev.* **D94** (2016) 094008, [1606.08030].